

Tip: this paper needs to be in conjunction with Lipinski paper. There are many references to lipinski here. Author said they were in communication with Lipinski

ARTICLE

 Check for updates

<https://doi.org/10.1038/s41467-021-21262-9> OPEN

# How $\mu$ -opioid receptor recognizes fentanyl

Quynh N. Vo  <sup>1,2</sup>, Paween Mahinthichaichan <sup>1,2</sup>, Jana Shen  <sup>2</sup>✉ & Christopher R. Ellis  <sup>1</sup>✉

Roughly half of the drug overdose-related deaths in the United States are related to synthetic opioids represented by fentanyl which is a potent agonist of mu-opioid receptor (mOR). In recent years, X-ray crystal structures of mOR in complex with morphine derivatives have been determined; however, structural basis of mOR activation by fentanyl-like opioids remains lacking. Exploiting the X-ray structure of BU72-bound mOR and several molecular simulation techniques, we elucidated the detailed binding mechanism of fentanyl. Surprisingly, in addition to the salt-bridge binding mode common to morphinan opiates, fentanyl can move deeper and form a stable hydrogen bond with the conserved His<sup>297</sup><sup>6.52</sup>, which has been suggested to modulate mOR's ligand affinity and pH dependence by previous mutagenesis experiments. Intriguingly, this secondary binding mode is only accessible when His<sup>297</sup><sup>6.52</sup> adopts a neutral HID tautomer. Alternative binding modes may represent a general mechanism in G protein-coupled receptor-ligand recognition.

challenge and purpose

general idea: H297 super important, authors want to module the ligand affinity and pH dependence to understand the binding mechanism of fentanyl.

What is the incorporation of HID/HIE/HIP?

<sup>1</sup> Center for Drug Evaluation and Research, United State Food and Drug Administration, Silver Spring, MD, USA. <sup>2</sup> Department of Pharmaceutical Sciences, University of Maryland School of Pharmacy, Baltimore, MD, USA. ✉email: [jana.shen@rx.umaryland.edu](mailto:jana.shen@rx.umaryland.edu); [christopher.ross.ellis@gmail.com](mailto:christopher.ross.ellis@gmail.com)

Opioids are highly effective pain relievers, but their addictive nature can easily lead to abuse and overdose-related deaths. From 1999 to 2018, almost 450,000 people died from opioid overdose in the United States<sup>1</sup>. Overdose deaths from synthetic opioids, represented by fentanyl and its derivatives, are now associated with more deaths than any other type of opioid<sup>2</sup>. The surge in fentanyl is attributed to high potency (50–400 times more potent than the naturally occurring morphine), fast onset, straightforward synthesis, and low-cost production<sup>3–6</sup>. Additionally, the fentanyl core is readily modified creating a vast chemical space of fentanyl analogs with abuse potential<sup>7</sup>.

Fentanyl and morphine opioids produce strong analgesic responses through binding and subsequent activation of a class A G protein-coupled receptor (GPCR)  $\mu$ -opioid receptor (mOR)<sup>8</sup>. In recent years, high-resolution crystal structures of mOR in complex with the morphinan agonist BU72<sup>9</sup>, antagonist  $\beta$ -FNA<sup>10</sup>, as well as the endogenous peptide analog agonist DAMGO<sup>11</sup> have been determined, featuring a salt bridge between a charged amine group of the ligand and a conserved residue Asp147 on the transmembrane helix (TM) 3 (Asp<sup>3,32</sup> in the Ballesteros-Weinstein numbering<sup>12</sup>) of mOR (Fig. 1a). The morphinan compounds and peptide analog also interact with a conserved His297 on TM6 (His<sup>6,52</sup> in the Ballesteros-Weinstein numbering<sup>12</sup>) via water-mediated hydrogen bonds. Mutagenesis studies demonstrated that mutation of either Asp147 or His297 as well as a reduced pH (which presumably protonates His297) decreases the binding affinities for DAMGO and naloxone (antagonist)<sup>13–15</sup>.

Despite the importance, surprisingly little is known about the signaling mechanism of fentanyl and how it interacts with mOR to illicit analgesic response<sup>6</sup>. It is conceivable that fentanyl and its analogs bind and activate mOR in the same manner as

morphinan compounds; however, the structural basis remains lacking. The aforementioned mutagenesis experiments performed to probe the role of Asp147 and His297 were inconclusive due to excessive non-specific binding of fentanyl<sup>15</sup>. Docking<sup>16,17</sup> and long-timescale molecular dynamics (MD) simulations<sup>18</sup> based on the docked structure of fentanyl in mOR confirmed the stability of the orthosteric binding mode involving the salt bridge with Asp147; however, the role of His297 has not been explored (Fig. 1).

Towards understanding the molecular mechanism of mOR activation by fentanyl, here we elucidate the detailed fentanyl-mOR binding mechanism by exploiting a morphinan-bound mOR crystal structure and several molecular dynamics (MD) methods, including the weighted ensemble (WE) approach<sup>19–21</sup> for enhanced path sampling and membrane-enabled continuous constant-pH MD (CpHMD) with replica-exchange<sup>22–24</sup>. The latter method has been previously applied to calculate  $pK_{a,b}$  and describe proton-coupled conformational dynamics of membrane channels<sup>25</sup> and transporters<sup>23,26,27</sup>. Surprisingly, WE path sampling found that when His297 adopts the HID tautomer, fentanyl can move deeper into the mOR and establish an alternative binding mode through hydrogen bonding with His297. CpHMD titration showed that His297 favors the HIE tautomer in the apo mOR; however, interaction with the piperidine amine of fentanyl locks it in the HID tautomer. Additional microsecond equilibrium simulations were conducted to further verify the two binding modes and generate fentanyl-mOR interaction fingerprints. Alternative binding modes and involvement of tautomer states may represent general mechanisms in GPCR-ligand recognition. Our work provides a starting point for understanding how fentanyl activates mOR at a molecular level. Fentanyl analogs that can be significantly more

the whole conclusion in these two sentences.

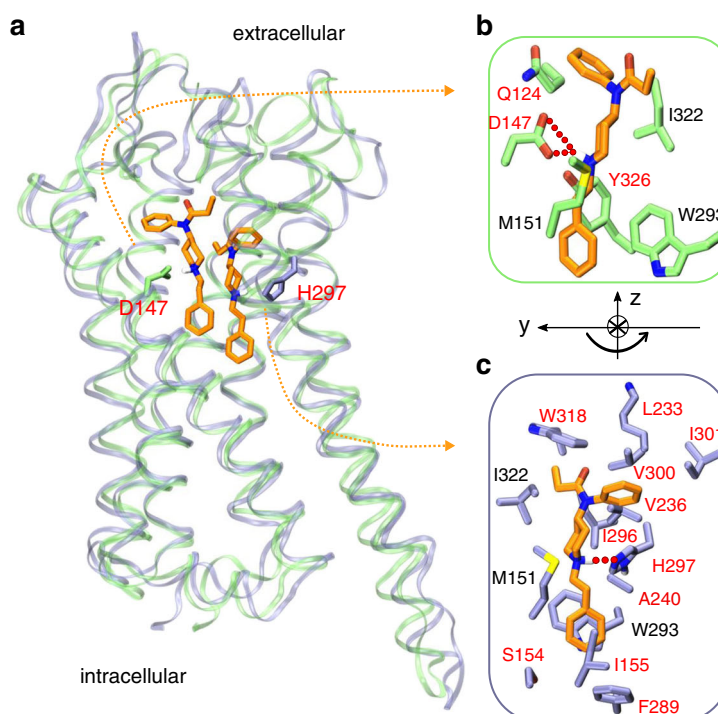


**Fig. 1 Fentanyl binding with mOR.** **a** Overlay of the representative simulation snapshots showing mOR is bound to fentanyl in the D147- (green) and H297- (purple) binding modes. **b** Zoomed-in view of the D147-binding mode, in which the charged piperidine amine of fentanyl forms a salt bridge with Asp147. **c** Zoomed-in view of the H297-binding mode, where the piperidine amine donates a proton to Ne of HID297. The curved arrow illustrates the change in the orientation of fentanyl in going from D147- to H297-binding mode. mOR residues making significant contacts with fentanyl (fraction greater than 0.5) are shown (see Fig. 4). Those unique to the two binding modes are labeled in red and otherwise in black. **d** Structure of fentanyl with different substituent groups and the protonated/charged amine labeled. **e** Histidine protonation states. HID and HIE are neutral while HIP is charged.

**Table 1 Summary of simulations in this work.**

two questions they want to know:  
 1) which starting configuration is better? more interaction? etc  
 2) which Histidine better resemble this biological system?

Simulation	Type	Starting configuration	H297 State	Time (μs)
		Binding mode		
WE-HIE	WE	D147 salt bridge	HIE	24.3
WE-HID	WE	D147 salt bridge	HID	23.6
CpH-apo	CpHMD	Apo active mOR	Dynamic	0.32
CpH-D147	CpHMD	D147 salt bridge	Dynamic	0.32
CpH-H297	CpHMD	H297 hydrogen bond	Dynamic	0.32
MD-D147(HID)	equil. MD	D147 salt-bridge	HID	0.5
MD-D147(HIE)	equil. MD	D147 salt-bridge	HIE	0.5
MD-D147(HIP)	equil. MD	D147 salt-bridge	HIP	0.5
MD-H297(HID)	equil. MD	H297 h-bond	HID	1.0
MD-H297(HIE)	equil. MD	H297 h-bond	HIE	1.0
MD-H297(HIP)	equil. MD	H297 h-bond	HIP	1.0

potent and addictive are emerging on the dark market at a rapid pace. The molecular mechanism by which structural modifications alter fentanyl potency and abuse potential can inform the design of safer analgesics to combat the opioid crisis.

Definitely a great way to close of introduction by restating the purpose.

## Results

**Fentanyl unbinds from the D147-bound configurations in the presence of HIE297.** Following the 115-ns MD to relax the docked fentanyl-mOR complex (details see Methods and Protocols and Supplementary Fig. 1), we performed WE all-atom MD simulations to explore the detailed binding interactions of fentanyl in mOR (Table 1). The fentanyl RMSD was used as the progress coordinate. The MD trajectories were produced using the GPU-accelerated PMEMD engine in AMBER18<sup>28</sup> and the Python-based WESTPA tool<sup>20</sup> was used to control the WE protocol.

In the first WE simulation of 24 μs aggregate time, His297 was fixed in the HIE tautomer (Ne atom of imidazole is protonated), as in the recent mOR simulations by the Dror group<sup>9,11</sup>. The WE-HIE simulation proceeded as expected. In the first 75 iterations or 2.5 μs of cumulative sampling time, fentanyl's piperidine stays near Asp147, sampling both the salt-bridged and solvent-separated configurations, with the FEN-D147 distance (minimum heavy-atom distance between the piperidine amine and the carboxylate) below 5 Å (Fig. 2a and Supplementary Fig. 2). During this time, fentanyl ΔZ fluctuates between 7.5 and 10.5 Å, and RMSD stays below 4 Å (Supplementary Fig. 2). ΔZ is defined as the distance between the centers of mass of fentanyl and mOR in the z direction, whereby the N- (52–65) and C-terminal (336–347) residues of mOR were excluded from the calculation. After 75 iterations, fentanyl starts to move upward and away from Asp147; after about 140 iterations or 8 μs of cumulative sampling time, RMSD increases to above 7.5 Å and ΔZ starts to sample values above 14 Å, indicating that fentanyl is on the way to exit mOR (Supplementary Fig. 2). At the end of 300 iterations or 24 μs of cumulative sampling time, fentanyl reaches the extracellular end of mOR (Supplementary Fig. 2). It is noteworthy that in the WE-HIE simulation, the FEN-H297 distance from the piperidine nitrogen to the unprotonated imidazole nitrogen is always above 4 Å, indicating that fentanyl's piperidine does not form hydrogen bond interactions with His297 (Fig. 2a and Supplementary Fig. 2). Interestingly, even with the intact piperidine-D147 salt bridge, fentanyl can sample various configurations with a RMSD as high as 8 Å (Supplementary Fig. 2).

**Fentanyl samples both D147- and H297-bound configurations in the presence of HID297.** In addition to HIE, a neutral histidine can adopt the HID tautomer state, whereby the Nδ atom is

protonated. Considering the important and yet unclear role of His297 in opioid-mOR binding, we conducted another WE simulation with His297 fixed in HID (WE-HID). Surprisingly, fentanyl did not exit mOR as was observed in the WE-HIE simulation. After about 27 iterations or 0.6 μs of cumulative sampling time, some of the trajectories start to sample configurations in which fentanyl laterally rotates 120°, translates 2 Å, and moves down 1 Å, enabling the formation of a stable hydrogen bond between the piperidine amine and the unprotonated Ne atom of HID297, (Figs. 1a, 2b, and Supplementary Fig. 3). At the same time, the RMSD remains below 7 Å. Unexpectedly, after about 210 iterations or 13 μs of cumulative sampling time, some trajectories start to sample configurations in which fentanyl is inserted deeper into the receptor (Supplementary Fig. 3). At the end of 20 μs aggregate time, fentanyl continues to sample the D147- and HID297-bound configurations along with positions in which it does not interact with either residue (Fig. 2b and Supplementary Fig. 3); however, the fentanyl ΔZ stay below 14 Å, indicating that it remains inside of the ligand accessible vestibule of mOR (Fig. 2b and Supplementary Fig. 3).

**Further comparison between the configurations from the WE-HIE and WE-HID simulations.** To further understand the differences in the configuration space sampled by fentanyl in the presence of HIE297 and HID297, we plotted FEN-H297 vs. FEN-D147 distance and color coded the data points by ΔZ of fentanyl. Corroborating with the previous analysis, these plots show that while the D147-bound configurations (FEN-D147 distance ≤ 3.5 Å) are sampled in both WE-HIE and WE-HID simulations, the H297-bound configurations (FEN-H297 distance ≤ 3.5 Å) are only sampled in the WE-HID simulation (Fig. 2c, d). Further, the H297-bound configurations sample lower ΔZ positions of 3–8 Å, as compared to the D147-bound configurations whereby ΔZ is in the range of 7–13 Å, (Fig. 2c-f, and Supplementary Fig. 2, 3). Interestingly, the WE-HID simulation also sampled fentanyl configurations deeply embedded in mOR (ΔZ ≤ 3 Å) but without a hydrogen bond with HID297 (FEN-H297 distance of 4–6 Å), suggesting that the piperidine-HID297 hydrogen bond may not be the only stabilizing factor for the deep insertion of fentanyl in mOR (Fig. 2d and Supplementary Fig. 4). Representative snapshots suggest that the interactions between the phenylethyl group and Trp293 may be a contributor (Fig. 2f).

**His297 favors the HIE tautomer in the apo mOR but the piperidine-HID297 interaction locks His297 in the HID state.** The WE simulations suggest that fentanyl has an alternative binding mode which may be promoted by the presence of the

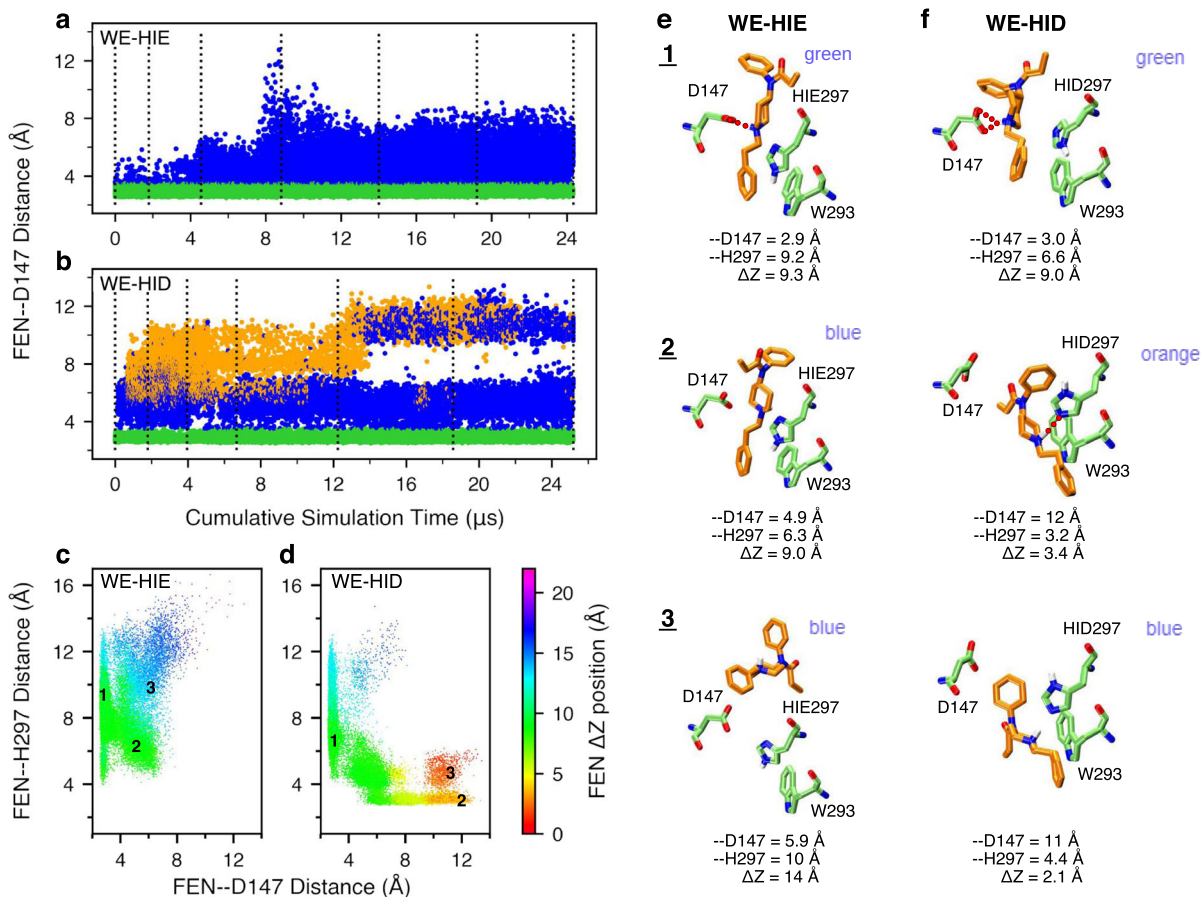


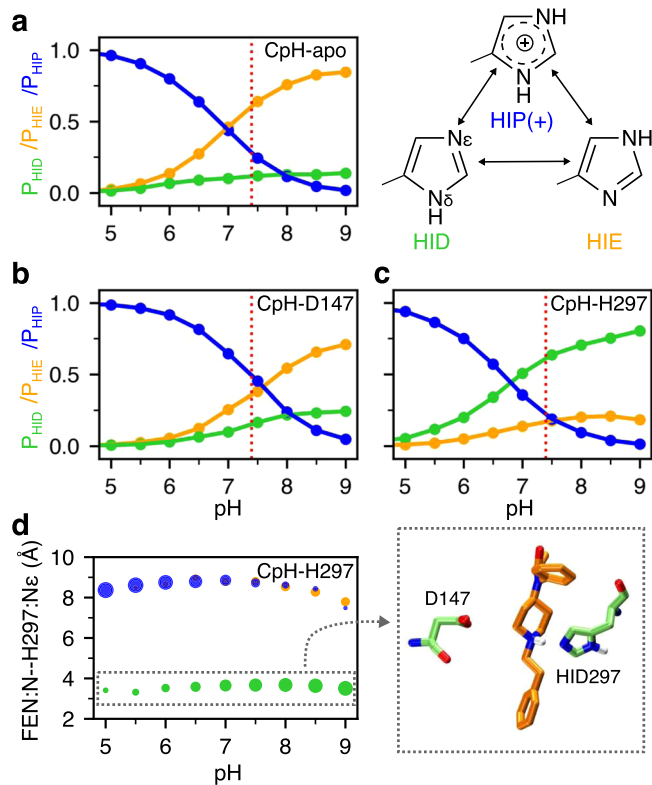
**Fig. 2 Fentanyl visits the D147-binding mode in the presence of HIE297 but both D147- and H297-binding modes in the presence of HID297.** **a, b** The FEN-D147 distance, referred to as the minimum distance between the piperidine nitrogen and the carboxylate oxygen of Asp147, as a function of the cumulative WE simulation time in the presence of HIE297 (**a**) or HID297 (**b**). Data with the FEN-D147 and FEN-H297 distances below 3.5 Å are colored green and orange, respectively, and otherwise blue. The unweighted data from all bins were taken and the time refers to the cumulative time. The dotted vertical lines are drawn at every 50 WE iterations. **c, d** FEN-H297 vs. FEN-D147 distance from the WE-HIE (**c**) and WE-HID (**d**) simulations. The data points are color coded by the fentanyl  $\Delta Z$  position, defined as the distance between the centers of mass of fentanyl and mOR in the z direction, whereby the N- (52–65) and C-terminal (336–347) residues of mOR were excluded from the calculation. The FEN-H297 distance is measured between the piperidine nitrogen and the unprotonated imidazole nitrogen of His297. Three groups of data (labeled in the plots) taken from the last 50 iterations of each simulation were subjected to the hierarchical clustering analysis. For WE-HIE, the three groups were defined as FEN-D147 distance  $\leq$  3.5 Å; FEN-D147 distance  $\geq$  4 Å and FEN-H297 distance  $\leq$  8 Å; and FEN-D147 distance  $\geq$  4 Å and FEN-H297 distance  $\geq$  8 Å. For WE-HID, the three groups were defined as FEN-D147 distance  $\leq$  3.5 Å; FEN-H297 distance  $\leq$  3.5 Å, and FEN-D147 distance  $\geq$  8.5 Å and FEN-H297 distance  $\geq$  4 Å. **e, f** Representative structures of the most populated clusters from the WE-HIE (**e**) and WE-HID (**f**) data defined in (**c**) and (**d**). The FEN-D147 and -H297 distances and the fentanyl  $\Delta Z$  position are given.

HID tautomer of His297. To determine the physiological relevance, we carried out titration simulations using the membrane-enabled hybrid-solvent CpHMD method with pH replica exchange<sup>22,23</sup> to determine the protonation state of His297 under physiological pH for the apo mOR and the fentanyl-bound mOR in the D147- as well as the H297-binding modes (Table 1). For each system, 16 pH replicas were simulated in the pH range 2.5–9.5, with the aggregate sampling time of 320 ns. All Asp/Glu/His and fentanyl's piperidine amine in the holo systems were allowed to titrate. The calculated  $pK_a$  of His297 is well converged (Supplementary Fig. 4).

In the absence of ligand (CpH-apo simulation), the calculated macroscopic  $pK_a$  of His297 is 6.8. At physiological pH 7.4, the HIE tautomer is predominantly sampled at 64%, while the HID tautomer and the charged HIP populations are 12% and 24%, respectively (Fig. 3a). The presence of fentanyl in the D147-binding mode upshifts the His297  $pK_a$  to 7.3 (CpH-D147 simulation). At physiological pH, both HIE and HIP are the predominant forms accounting for 39% and 44% of the

population, respectively, while HID accounts for 17% of the population (Fig. 3b).

Finally, CpHMD titration was also performed for the fentanyl-mOR complex in the H297-binding mode (CpH-H297 simulation). Interestingly, the calculated  $pK_a$  of His297 is 6.7, nearly the same as for the apo mOR; however, at physiological pH HID is the predominant form with a population of 60%, while the HIE and HIP forms account for 20% each. Importantly, the protonation state of His297 is coupled to its distance to the piperidine amine of fentanyl (Fig. 3d). When the piperidine nitrogen is within 4 Å of the Ne atom of His297, the HID state is exclusively sampled, whereas the HIE and HIP states are only allowed when the piperidine–His297 distance is  $\geq$  7 Å (Fig. 3d). These data are consistent with the equilibrium MD which shows that the distance is  $3.0 \pm 0.22$  Å,  $7.4 \pm 0.72$  Å, and  $8.0 \pm 0.5$  Å with HID297, HIE297, and HIP297, respectively, while the distance range 4–7 Å is rarely sampled (Supplementary Fig. 8). Note, in both holo simulations the piperidine amine remains protonated/charged in the entire pH range 2.5–9.5.

**Fig. 3 Protonation state of His297 is influenced by fentanyl binding.**

**a–c** Occupancies of the HID (green), HIE (orange), and HIP (blue) states of His297 as a function of pH from the replica-exchange CpHMD simulations of the apo mOR (**a**) and fentanyl-bound complex in the D147- (**b**) and H297-binding mode (**c**). The three states are in equilibrium through protonation/deprotonation and tautomerization. **d** Average distance between the piperidine nitrogen and His297's Nε at different pH conditions when His297 is in the HID (green), HIE (orange), or HIP (blue) state. The area of the data point is proportional to the occupancy of the protonation state. A zoomed-in snapshot corresponding to the HID state is shown.

The CpHMD simulations demonstrate that ligand interaction perturbs the protonation state of His297: while the apo mOR preferably samples HIE297, the population of HIP or HID state may increase upon ligand binding. When fentanyl interacts with Asp147, the HIP state is sampled with an equal probability as HIE, and when fentanyl interacts with His297, HID is the preferred state. These data provide an explanation as to why the H297-binding mode (quickly) emerged in the WE simulation with HID297 but not HIE297.

**Asp114 is deprotonated.** The protonation state of the highly conserved residue Asp114 (Asp<sup>2,50</sup>) in the active mOR remains unclear to this day. Despite not having a direct role in ligand binding, Asp114 is involved in mOR activation.<sup>9,11,29,30</sup> Previous experiments<sup>30</sup> and simulations<sup>9,11,29</sup> demonstrated that Asp114 binds a sodium ion in the inactive but not active state of GPCRs. Based on the lack of sodium binding, two previous MD studies used a protonated Asp114<sup>9,11</sup>, while other published work did not specify the protonation state<sup>18,31,32</sup>. The CpHMD titration gave a  $pK_a$  of  $4.8 \pm 0.30$  for the apo and  $5.1 \pm 0.26/0.29$  for the fentanyl-bound mOR in the D147- or H297-binding mode. Therefore, even though the  $pK_a$ s are upshifted relative to solution value of 3.8<sup>33</sup>, Asp114 remains deprotonated at physiological pH in the active mOR according to the CpHMD simulations.

**The D147-binding mode is stable regardless of the protonation state of H297.** To further characterize fentanyl-mOR interactions and delineate the impact of the His297 protonation state, we carried out a series of equilibrium simulations (Table 1). First, three 0.5-μs simulations were initiated from the equilibrated fentanyl-mOR complex in the D147-binding mode with His297 fixed in the HID, HIE, and HIP states (Table 1). To quantify ligand-receptor interactions, the fractions of time for the mOR residues that form at least one heavy-atom contact with fentanyl were calculated (Fig. 4a-d, top panels). To determine what parts of fentanyl contribute to the receptor recognition, a fingerprint matrix was calculated which shows the contacts formed between specific mOR residues and fentanyl substituents (Fig. 4a-d, bottom panels). Simulations starting from the D147-binding mode demonstrated that many interactions are independent of the protonation state of His297. Most importantly, the piperidine-D147 salt bridge remains stable throughout the 0.5-μs trajectories with HIE297, HID297, and HIP297 (Supplementary Fig. 5 and Fig. 4a-c), consistent with the WE simulations. Interestingly, while maintaining the salt bridge with piperidine, Asp147 also interacts with phenyl and phenethyl at the same time (Fig. 4a-c, bottom panels), which may provide further stabilization to the D147-binding mode.

Another important fentanyl-mOR contact is the aromatic stacking interaction between the phenyl ring of the phenethyl group and Trp293 (Figs. 1b, 4a-c bottom panels, and Supplementary Fig. 6), which remains stable in all three simulations. The importance of the phenethyl group at this location in the 4-anilidopiperidine core of fentanyl is supported by the observations that substitution with methyl (as in N-methyl norfentanyl) increases the  $K_i$  value by about 40 fold<sup>34</sup>, and removal of one ethylene group renders the ligand inactive<sup>35</sup>. However, substitution with a different aromatic ring, e.g. thiophene in sufentanil and ethyl tetrazolone in alfentanil, does not appear to be have a significant effect on binding affinity, although the latter ligands have an O-methyl group at the 4-axial hydrogen position<sup>4</sup>. The importance of the phenethyl-Trp293 stacking interaction is also consistent with a recent study which showed that removal of one methylene group from phenethyl increases the  $IC_{50}$  value by two orders of magnitude<sup>36</sup>.

**Fentanyl-mOR interaction profiles vary with different protonation state of His297 albeit in the same D147-binding mode.** Despite the similarities, the fentanyl-mOR interaction profiles obtained from the simulations MD-D147(HID), MD-D147(HIE), MD-D147(HIP) show differences (Fig. 4a-c). To quantify the overall difference between two interaction profiles, the Tanimoto coefficient ( $T_c$ )<sup>37</sup> was calculated (Fig. 5a), where  $T_c$  of 1 indicates that identical mOR residues are involved in binding to fentanyl. Accordingly, the contact profiles with HIE297 and HIP297 are more similar ( $T_c$  of 0.81), whereas the contact profiles with HID297 and HIE297/HIP297 are somewhat less similar ( $T_c$  of 0.71/0.73). As to the latter, the most significant differences are in the N-terminus. While fentanyl makes no contact with the N-terminus in the simulation with HID297, it interacts via propanamide and phenyl groups with His54 and Ser55 in the simulations with HIE297/HIP297. The fentanyl-N-terminus interactions are consistent with an experimental study which demonstrated that truncation of the mOR N-terminus increases the dissociation constant of fentanyl by 30 fold<sup>38</sup>. Significant differences are also seen in the TM2 contacts between simulations with HIE297 and HID297/HIP297. Four TM2 residues, Ala113, Asp114, Ala117, Gln124, are involved in stable interactions with fentanyl in the simulations with HID297/HIP297; however, only one TM2 residue Gln124 contacts fentanyl in the

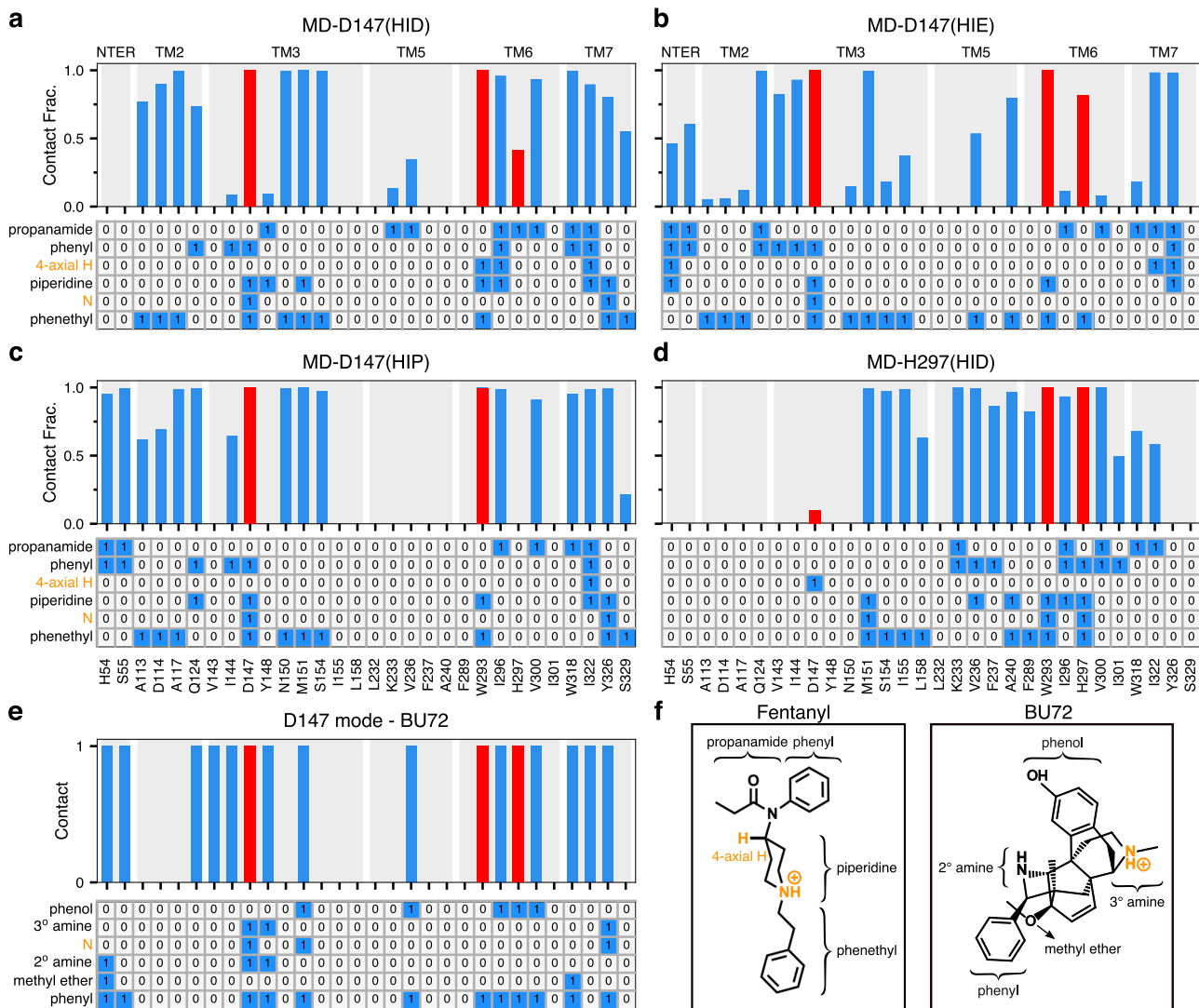


**Fig. 4 Fentanyl-mOR interaction profiles in the presence of different protonation state of His297 and comparison to the BU72-mOR contacts in the crystal structure.** **a-d** Top. Fraction of time that mOR residues form contacts with fentanyl in the equilibrium MD starting from the D147- (**a-c**) and H297-binding modes (**d**). A contact is considered formed if any sidechain heavy atom is within 4.5 Å of any fentanyl heavy atom. Only residues that form contacts for least 25% of the time in at least one of the six equilibrium simulations are shown. Contacts with Asp147, Trp293, and His297 are highlighted in red. **a-d** Bottom. Ligand-mOR fingerprint matrix showing the fentanyl groups as rows and mOR residue as columns. 1 represents in contact and 0 represents no contact. **e** mOR residues forming contacts with BU72 in the crystal structure (PDB: 5C1M<sup>9</sup>). **f** Chemical structure of fentanyl and BU72. Different substituent groups are labeled. The 4-axial hydrogen and amine nitrogen of the piperidine group are indicated.

simulation with HIE297 (Fig. 4a–c, top panels). A closer examination revealed that Gln124 interacts with phenyl in the simulation with HID297/HIP297 but it additionally interacts with propanamide in the simulation with HIE297, forming a stable hydrogen bond (Fig. 4a, b, bottom panels, Supplementary Fig. 7). This hydrogen bond may contribute to an upward shift of fentanyl's position in the simulation with HIE297 (see later discussion), resulting in a decrease of the aromatic stacking interaction between the phenyl ring of the phenethyl group and Trp293 (Supplementary Fig. 6).

**The H297-binding mode is stabilized by many fentanyl-mOR contacts in the presence of HID297.** To further evaluate the fentanyl-mOR interactions in the H297-binding mode, three 1-μs equilibrium simulations were initiated from the H297-binding mode with His297 fixed in the HID, HIE, and HIP states. We refer to these simulations as MD-H297(HID), MD-H297(HIE), and MD-H297(HIP), respectively (Table 1). In the MD-H297

(HID) simulation, the piperidine-H297 hydrogen bond remains stable; however, the hydrogen bond immediately breaks and the N–Ne distance fluctuates around 7.5 Å and 8.0 Å in the simulations with HIE297 and HIP297, respectively (Supplementary Fig. 8). These results are in agreement with the CpHMD titration, confirming that the H297-binding mode is only stable in the presence of HID297. In addition to the piperidine-H297 hydrogen bond, the simulation MD-H297(HID) shows that fentanyl forms stable contacts (with a contact fraction greater than 0.5) with over a dozen of residues on TM3, TM5, TM6, and TM7 (Figs. 1c, 4d), which explains the stability of the H297-binding mode in both MD-H297(HID) and WE-HID simulations.

**Comparison of the fentanyl-mOR contact profiles in the two binding modes.** Several interactions, e.g., stable contacts with Met151 (TM3), Trp293 (TM6), and Ile322 (TM7), are shared among all equilibrium simulations, regardless of the binding mode or His297 protonation state (Figs. 1b, c, 4a–d). Among

	MD-D147	MD-D147	MD-D147	MD-H297	D147 mode-BU72
(HID)	(HIE)	(HIP)	(HID)		
MD-D147	1				
(HIE)	0.71	1			
MD-D147	0.73	0.81	1		
(HIP)					
MD-H297	0.44	0.46	0.31	1	
(HID)					
D147 mode-BU72	0.57	0.71	0.57	0.38	1

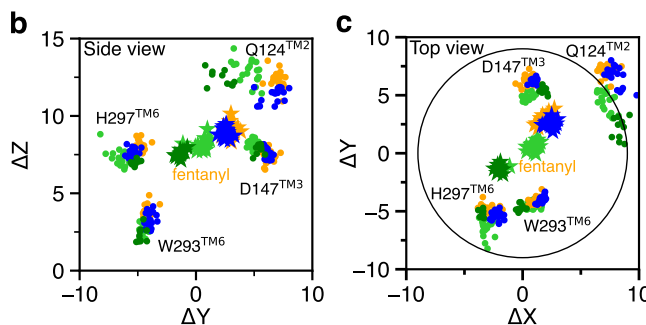
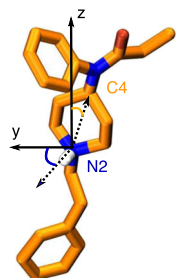


**Fig. 5 Contact similarity and spatial relationship between the D147- and H297-binding modes.** **a**, Tanimoto coefficients ( $T_c$ ) calculated using the binary contacts (details see Methods and Protocols).  $T_c$  ranges from 0 to 1, where 1 indicates identical mOR residues are involved in fentanyl binding in both simulations. **b, c**, Locations of fentanyl (stars) and critical amino acids (circles) plotted on the (Y,Z) and (X,Y) planes. Data points are sampled every 10 ns. The center of mass of mOR is set to origin. The data from MD-D147(HID), MD-D147(HIE), and MD-D147(HIP) are colored light green, orange, and blue, respectively, while the data from MD-H297(HID) are colored dark green. The z-axis is the membrane normal.

them is the aromatic stacking between the phenethyl group and Trp293 (Fig. 4a–d, Supplementary Fig. 6), which is stable in all simulations. Nonetheless, the contact profile from the simulation MD-H297(HID) is drastically different from those in the D147-binding mode. The  $T_c$  value comparing MD-H297(HID) with MD-D147(HID), MD-D147(HIE), and MD-D147(HIP) are 0.44, 0.46, and 0.31, respectively (Fig. 5a). Fentanyl contacts with the N terminus and TM2 residues are completely absent and fewer TM7 residues are involved in fentanyl interactions in the simulation MD-H297(HID) (Fig. 4d). Most contacts uniquely observed for the H297-binding mode involve TM5 residues. As His297 is slightly below Asp147, a switch from the piperidine–D147 salt bridge to the piperidine–H297 hydrogen-bond results in a lower vertical position for fentanyl as compared to the D147-binding mode. The change in the vertical position likely contributes to the differences in the mOR residues interacting with fentanyl.

The fentanyl–H297 interactions also appear to perturb the local environment. While the backbone amide–carbonyl hydrogen bond between His297 and Trp293 is present in all equilibrium simulations, the backbone carbonyl of Trp293 also accepts a stable hydrogen bond from the N $\delta$  atom of HID297 in the simulation MD-H297(HID) (Supplementary Fig. 7A, C). We hypothesize that the hydrogen-bond network (fentanyl–HID297–Trp293) together with the aromatic stacking between the phenethyl group and Trp293 contributes to a slight increase in the  $\chi_2$  angle of Trp293 ( $125 \pm 9^\circ$ ), as compared to that in the D147-binding mode simulations ( $112 \pm 10^\circ$  with HIE297,  $116 \pm 9.6^\circ$  with HID297, and  $110 \pm 9.5^\circ$  with HIP297). Interestingly, the  $\chi_2$  angle of Trp293 in

the X-ray structure of active mOR bound to BU72 (PDB: 5C1M<sup>9</sup>) is  $120^\circ$ , while that in the X-ray structure of the inactive mOR bound to the antagonist  $\beta$ -FNA (PDB: 4DKL<sup>10</sup>) is  $80^\circ$ .

Another intriguing feature of the simulation MD-H297(HID) is the transient contact between Asp147 and the 4-axial hydrogen of the piperidine ring (Fig. 4d, f). In the simulations of the D147-binding mode, the 4-axial hydrogen makes contact with TM6 or TM7 residues (Fig. 4a–c); however, in the simulation of the H297-binding mode, since the piperidine position is lower due to hydrogen bonding with His297, the 4-axial hydrogen position is also lowered, enabling an interaction with Asp147. Thus, we hypothesize that a substitution for a larger polar group at the 4-axial position might add stable interactions to both the D147- and H297-binding modes, which would potentially explain the increased binding affinity of fentanyl analogs with a methyl ester substitution at the 4-axial position, e.g. carfentanil and remifentanil<sup>3,34,36,39</sup>.

**Comparison of the position and conformation of fentanyl in different binding modes.** The WE simulations demonstrated that the two fentanyl binding modes are readily accessible from one another in the presence of HID297 (Fig. 2d). The equilibrium simulations found that fentanyl contacts His297 in the D147-binding mode with HID297 or HIE297 (Fig. 4a, b) and it transiently interacts with Asp147 in the H297-binding mode with HID297 (Fig. 4d). To quantify the spatial relationship between the two binding modes, we calculated the center of mass (COM) positions of fentanyl and key contact residues relative to that of mOR based on the equilibrium simulations of the D147- and H297-binding modes and plotted in the (Y,Z) and (X,Y) planes. The resulting side (Fig. 5b) and top (Fig. 5c) views of the fentanyl and mOR residue locations showed that fentanyl adopts a similar position in the simulations of the D147-binding mode with HIE297 or HIP297; however, intriguingly, with HID297, the fentanyl position is moved towards the position it takes in the simulation of the H297-binding mode. Specifically, in going from the D147- to the H297-binding mode, fentanyl laterally rotates by about  $120^\circ$  such that the piperidine amine faces the N $\epsilon$  atom of His297, and translates by about  $2 \text{ \AA}$  on the (X,Y) plane before moving down the Z-axis (Fig. 5b, c). The simulation MD-H297 (HID) gave the fentanyl  $\Delta Z$  of  $7.4 \pm 0.4 \text{ \AA}$ , as compared to  $8.3 \pm 0.4$ ,  $8.8 \pm 0.3$ , and  $9.2 \pm 0.5$  from the simulations MD-D147(HID), MD-D147(HID), and MD-D147(HIP), respectively. Additionally, fentanyl is in a more upright position in the simulation of the H297 binding mode, with a vertical angle of  $15^\circ$ , compared to the angle of  $20\text{--}40^\circ$  in the simulations of the D147-binding mode (Supplementary Fig. 10).

A closer look at the conformation of His297 suggests that its  $\chi_2$  dihedral angle may be modulated by the protonation/tautomer state (Supplementary Fig. 11). When His297 is in the HIE or HIP state, only the negative  $\chi_2$  angle is sampled regardless of the binding mode; however, in the presence of HID297, the simulation of the D147-binding mode samples both negative and positive  $\chi_2$  angles, whereas the simulation of the H297-binding mode only samples the positive  $\chi_2$  angle. Thus, it is possible that HID297 allows both rotameric states, while the piperidine–H297 hydrogen bond locks the angle at  $100^\circ$ . These data further support the notion that the two binding modes are made accessible to one another in the presence of HID297.

**Comparison to the crystal structures of mOR in complex with BU72 and other ligands.** Finally, we compare the two fentanyl binding modes to the crystal structure of the BU72-bound mOR, which was used as a template to build the initial structure of fentanyl–mOR complex for WE simulations. The BU72-mOR

binding profile is most similar to fentanyl's D147-binding profile in the presence of HIE297 ( $T_c$  of 0.71) due to their nearly identical interactions with the N-terminus, TM2, TM3 and TM7. To a lesser extent, the BU72 binding profile shares similarities with fentanyl's D147-binding profile in the presence of HID297 or HIP297 ( $T_c$  of 0.57 for both). Importantly, the six residues, Gln124 (TM2), Asp147 and Met151 (TM3), Trp293 (TM6), Ile322 and Tyr326 (TM7), which form the foundation of the D147 binding pocket for fentanyl (with contact fraction greater than 0.5 regardless of the protonation state of His297) are present in the BU72-mOR binding contacts (Fig. 4a-c). In contrast, the BU72-mOR contact profile has a much lower overlap with fentanyl's H297-binding profile ( $T_c$  of 0.38). In addition to BU72, we compare fentanyl's D147-binding profile (HIE297) to DAMGO- and  $\beta$ -FNA contacts with mOR based on the crystal structures (Supplementary Fig. 13). In contrast to fentanyl and BU72, DAMGO (a natural agonist) and  $\beta$ -FNA (an antagonist) do not form contacts with TM2 in the crystal structures. Other than that, DAMGO-mOR contact profile is similar to BU72-mOR and fentanyl's D147-binding profile (with HIE297), whereas  $\beta$ -FNA makes additional contacts with TM6 (Ala287, Ile290, and Val291) and has different contacts with TM7.

## Discussion

In summary, several molecular dynamics simulation techniques have been applied to investigate fentanyl binding to mOR. The WE simulations confirmed that fentanyl binds to mOR via the salt-bridge interaction between the piperidine amine and the conserved Asp147, consistent with the X-ray crystal structures of mOR in complex with BU72,  $\beta$ -FNA, and DAMGO<sup>9–11</sup>. However, surprisingly, when His297 is protonated at  $\delta$  nitrogen (HID), fentanyl can also adopt a H297-binding mode, in which the piperidine amine donates a hydrogen bond to the  $\epsilon$  nitrogen of HID297. The conventional single trajectory simulations confirmed that the D147-binding mode is stable regardless of the protonation state of His297, whereas the H297-binding mode is only compatible with HID297. These findings are consistent with a recent conventional MD study of the fentanyl-mOR binding, which found that the D147 binding mode was stable in the presence of HID297<sup>18</sup> but fentanyl moved deeper to contact HID297 in some trajectories (personal communication with Lipiński). Our CpHMD titration rationalized the finding by showing that in the absence of the piperidine amine-imidazole interaction, His297 can titrate via either N $\delta$  or N $\epsilon$ ; however, in the presence of the interaction, N $\epsilon$  loses the ability to gain a proton, locking histidine in the HID form.

We note that the calculation of the relative stability of the D147- vs. H297-binding mode is beyond the scope of the present work. Such a study would require converged WE simulations and accurate force field for quantifying the strengths of salt bridges and hydrogen bonds. Previous work by us<sup>25</sup> and others<sup>40</sup> showed that the CHARMM36<sup>41</sup> or the CHARMM36m force field<sup>42</sup> used in this work overstabilizes salt bridges formed by aspartates, although this might not be the case for the piperidine-Asp147 interaction. Overstabilization of salt bridges is a common problem with additive force fields, which may be overcome by explicit or implicit consideration of polarization<sup>40</sup>. We also note that given converged WE simulations, the transition rate between the two binding modes may be estimated<sup>43</sup>, which is a topic of future exploration.

It is important to consider the physiological relevance of the H297-binding mode. According to the CpHMD titration, at physiological pH, HIE297 is the predominant form in the apo mOR, and HID297 is least populated in both the apo and holo mOR in the D147-binding mode. Consistent with these data, the

crystal structure-based BU72-mOR contact profile bears the strongest resemblance to the simulated D147-binding mode with HIE297 as compared to HID297 or HIP297. Thus, we hypothesize that fentanyl primarily binds mOR via the D147 mode under physiological pH, while the H297-binding mode is a secondary state. This hypothesis is consistent with the recent experiments<sup>15,44,45</sup> showing that acidic pH has a negligible effect on fentanyl-mOR binding. These experiments also showed that fluorinated fentanyl which have lower p $K_a$ s (6.8–7.2) than fentanyl (~8.9<sup>46,47</sup>) have increased affinities for mOR at lower pH. The CpHMD simulations showed that fentanyl's piperidine amine remains protonated/charged up to pH 9.5, while Asp147 is deprotonated with an estimated p $K_a$  of 3–4. Thus, our data are consistent with the hypothesis<sup>44,45,48</sup> that while fentanyl's D147-binding is not affected, lowering pH promotes protonation of the fluorinated fentanyls and thereby strengthening the salt bridge with Asp147. We expect the fluorinated fentanyls to have a lower potential for the His297-binding mode at physiological pH than fentanyl due to the decreased protonation of the piperidine.

The X-ray structures of mOR in complex with BU72,  $\beta$ -FNA, and DAMGO<sup>9–11</sup> show that while the piperidine amine forms a salt bridge with Asp147, the phenol hydroxyl group of the ligand forms a water-mediated hydrogen bond with His297. MD simulations of Dror and coworkers confirmed the stability of the water-mediated interactions between BU72 or DAMGO and His297 (HIE)<sup>9,11</sup>. Simulations of Carloni and coworkers<sup>31</sup> found that while in the D147-binding mode, the phenol group of morphine or hydro-morphone forms a direct or water-mediated hydrogen bond with His297 (HIE), respectively. Morphine was also suggested to make hydrophobic contacts with His297 (HID) while in the D147-binding mode by the recent MD study of Lipiński and Sadlej<sup>18</sup>. The de novo binding simulations of the Filizola group<sup>32</sup> showed that oliceridine (TRV-130) which has an atypical chemical scaffold binds mOR via water-mediated interactions with Asp147, while frequently contacting His297 (protonation state unclear). Fentanyl does not have a phenol group, and it differs from morphinan ligands in several other ways. Fentanyl has an elongated shape; it is highly flexible with at least seven rotational bonds; and it has only two structural elements capable of forming hydrogen bonds (amine and carbonyl groups). In contrast, morphinan ligands are bulkier, rigid, and possess more structural elements (i.e. phenol group) with hydrogen bonding capabilities. The bulkier structure and additional hydrogen-bond interactions may further stabilize the piperidine-D147 salt bridge, preventing the ligand from moving deeper into mOR and access the H297-binding mode. Therefore, it is possible that the H297-binding mode is unique to fentanyl and analogs. Intriguingly, a combined MD and experimental study found that unlike synthetic antagonists, the endogenous agonist acetylcholine (a small elongated molecule) can diffuse into a much deeper binding pocket of M3 and M4 muscarinic acetylcholine receptors<sup>49</sup>. Thus, alternative binding modes may be a general phenomenon of GPCR-ligand recognition.

The CpHMD titration allowed us to determine the protonation states of His297 and all other titratable sites in mOR, including the conserved Asp114<sup>2,50</sup>. Sodium binding in the inactive mOR suggests a deprotonated Asp114<sup>30</sup>, while the protonation state for the active mOR remains unclear. Recently, the p $K_a$  of the analogous Asp<sup>2,50</sup> in M2 muscarinic acetylcholine receptor (m2R) was calculated using the Poisson-Boltzmann method with a protein electric constant of 4<sup>50</sup>. The calculation gave a p $K_a$  of 8–12 when sodium is 5 Å away from Asp<sup>2,50</sup>. However, it is widely known that the continuum-based Poisson-Boltzmann methods overestimate the p $K_a$ s of internal residues, particularly with a low dielectric constant (e.g. 4)<sup>51</sup>. The CpHMD simulations estimated the p $K_a$ s of 4.8–5.1 for the apo and fentanyl-bound mOR, thus suggesting that it remains deprotonated in the active mOR.

does that mean it also binds to sodium ion in active?

They are saying that there are two neutral tautomer and it is not wrong to have one over the other because all 3 protonation stats may be sampled at pH 7.4 ir.

They just want to tell you that a certain tautomer may alter the mechanism and thermodynamics of ligand binding.

Having a solution  $pK_a$  of 6.5<sup>33</sup> and two neutral tautomer forms, histidine may sample all three protonation states in the protein environment at physiological pH 7.4. Our work demonstrates that the tautomer state of histidine in the ligand access region may alter the mechanism and possibly also the thermodynamics and kinetics of ligand binding. Thus, the conventional treatment in MD simulations, i.e., fixing histidine in a neutral tautomer state following the program default (HIE in Amber<sup>28</sup> and HID in CHARMM-GUI<sup>52</sup>) may not be appropriate for detailed investigations.

**more limitations** A caveat of the study is that all other histidines have been fixed in one protonation state in the WE and equilibrium simulations, even though some of them may sample alternative protonation state at physiological pH according to the CpHMD titration. A more complete understanding of how protonation states impact the conformational dynamics and ligand binding of GPCRs awaits the development of GPU-accelerated hybrid-solvent<sup>22,23</sup> and all-atom CpHMD methods<sup>53</sup> and their integration with enhanced sampling protocols such as the WE approach<sup>19,21,54</sup>. We also note that the present work is based on the activated structure of mOR and does not explore the large conformational changes of the receptor, which likely occur on a much slower timescale, e.g., the activation time of the class A GPCR  $\alpha_{2A}$  adrenergic receptor was estimated as 40 ms<sup>55</sup>. Notwithstanding the caveats, our detailed fentanyl-mOR interaction fingerprint analysis provides a basis for pharmacological investigations of fentanyl analogs, particularly how structural modifications alter the binding properties of fentanyl derivatives which may have increased potency and abuse potential.

## Methods

All fixed-charge simulations (weighted ensemble and equilibrium molecular dynamics) were carried out using the GPU-accelerated *pmemd* engine in AMBER18<sup>28</sup>. The continuous constant pH molecular dynamics (CpHMD) simulations were carried out with the CHARMM program (version c42)<sup>56</sup>. The protein was represented by CHARMM36m<sup>41</sup> and CHARMM22/CMAP force fields<sup>57,58</sup> in the fixed-charge and CpHMD simulations, respectively. Water was represented by the CHARMM-style TIP3P force field.<sup>56</sup> The POPC and cholesterol molecules were represented by the CHARMM36 lipid force field<sup>59</sup>. The force field parameters for fentanyl were obtained using the ParamChem CGENFF server<sup>60</sup>.

**Equilibration simulation of apo active mOR in a lipid bilayer.** The X-ray crystal structure of mOR in complex with BU72 (PDB ID: 5C1M)<sup>9</sup> was used as the starting model for apo active mOR. The crystal structure represents the wild type but contains a cysteine-s-acetamide (YCM) at position 57. This residue was converted to a cysteine (Cys57). A cholesterol molecule was resolved in the X-ray structure and is bound to the extracellular leaflet near TM7. This cholesterol and all crystal waters in the interior of mOR were kept. Seven additional water molecules were added using the DOWSER program<sup>61</sup>. Apo mOR was oriented with respect to membrane using the OPM (Orientations of Proteins in Membranes) database<sup>62</sup>. The CHARMM-GUI web server<sup>52</sup> was then used to construct the system of mOR embedded in a POPC (1-palmitoyl-2-oleoyl-glycero-3-phosphocholine) lipid bilayer. The disulfide bond observed in the crystal structure was imposed between Cys140 and Cys217. All titratable residues were fixed in the standard protonation states. All histidine residues were set to the neutral N<sub>8</sub> tautomer (HID) as in the default setting of CHARMM<sup>56</sup>. The system was first energy minimized using the steepest descent followed by conjugate gradient algorithm. The system was then gradually heated from 0 to 310 K over 200 ps with harmonic restraints on the protein heavy atoms, lipids and bound water molecules (same as Step 1 in Supplementary Table 1). Following heating, the system was equilibrated for 117 ns, during which time the various harmonic restraints were gradually reduced to zero (Supplementary Table 1). The final dimension of the system was  $\sim 87 \times 87 \times 113 \text{ \AA}^3$ . The final snapshot was used for constructing the fentanyl-bound mOR model and as the starting structure for the replica-exchange CpHMD simulations of apo mOR (CpH-apo).

**Relaxation of the docked fentanyl-mOR complex in a lipid bilayer.** The fentanyl-bound mOR model was prepared by superimposing a top fentanyl binding pose from a previous docking study<sup>16</sup> onto the final snapshot from the aforementioned equilibration simulation of apo active mOR. The docked pose showed a salt bridge between the piperidine nitrogen and Asp147 and an aromatic stacking between the phenethyl ring and His297. The docked model was equilibrated for 115 ns, using harmonic restraints imposed on the protein and fentanyl heavy atoms

in the first 5 ns (details see Supplementary Table 2). During the unrestrained part of the simulation, the root-mean-square deviation (RMSD) of the fentanyl heavy-atom positions with respect to the docked structure steadily increases in the first 20 ns and stabilizes at about 6 Å in the remainder of the 110 ns simulation (Supplementary Fig. 1). Concomitant with the fentanyl RMSD increase, the minimum distance between fentanyl's piperidine nitrogen and His297's imidazole nitrogen decreases from 10 to about 7 Å (Supplementary Fig. 1); however, the salt bridge between the positively charged piperidine amine and the negatively charged Asp147 remains largely stable except for occasional excursions (Supplementary Fig. 1), consistent with a previous  $\mu$ s simulation study<sup>18</sup>. The final snapshot was used as the starting configuration for the WE simulations.

**Weighted ensemble MD simulations.** Weighted ensemble (WE) is a path sampling protocol that uses splitting and merging trajectories to enhance sampling of rare events. Briefly, the configuration space is divided into bins based on a pre-determined progress coordinate and a fixed number of walkers (trajectories) per bin is targeted. At the beginning of the simulation, walkers are initiated from a single bin and after a specified time interval, resampling is performed by evaluating the number of walkers per bin, and for bins with less than desired number of walkers, the walker is replicated (or split), and for bins with more than desired number of walkers, the walkers are pruned. Thus, over time, more bins are sampled and the simulation progresses along the progress coordinate. Details theory and algorithm can be found elsewhere<sup>19,21,54</sup>.

Two WE MD simulations were carried out starting from the equilibrated fentanyl-mOR complex structure, with His297 fixed in either HIE (WE-HIE) or HID (WE-HID) state. The Python-based tool WESTPA<sup>54</sup> was used to control the WE protocol and data storage. The root-mean-square deviation (RMSD) of the fentanyl heavy-atom positions with respect to their starting positions was used as the progress coordinate. The configuration space was divided into bins that covered the RMSD values of 0 and 10 Å. A target number of four and five walkers per bin was used for the WE-HIE and WE-HID simulations, respectively. The fixed time interval for resampling of each walker was 0.5 ns. The bin widths were changed manually in the beginning of the simulations to further accelerate sampling, and the final bin boundaries were placed at the following RMSD values: 0, 0.5, 1, 1.25, 1.5, 1.75, 2, 2.1, 2.2, 2.3, 2.4, 2.5, 2.6, 2.7, 2.8, 2.9, 3, 3.1, 3.2, 3.3, 3.4, 3.5, 3.6, 3.7, 3.8, 3.9, 4, 4.1, 4.2, 4.3, 4.4, 4.5, 4.6, 4.7, 4.8, 4.9, 5, 5.25, 5.5, 5.75, 6, 6.25, 6.5, 6.75, 7, 7.25, 7.5, 7.75, 8, 8.25, 8.5, 8.75, 9, 9.5, 10, >10. The WE simulations employed the Langevin thermostat, as a stochastic thermostat is required for the WE strategy to generate continuous pathways with no bias in the dynamics. A total of about 300 iterations were conducted for WE-HIE and WE-HID simulations. From the WE-HID simulation, we uncovered an alternative binding mode that involved a hydrogen bond between fentanyl's piperidine nitrogen and His297's Ne. The bound pose was used as the starting configuration for the equilibrium simulation MD-H297(HID). To prepare the starting configurations for the equilibrium simulations MD-H297(HIE) and MD-H297(HIP), the protonation state of His297 in the bound pose was switched followed by 65 ns equilibration (Supplementary Table 3). The final snapshot which no longer contained the piperidine-H297(NE) hydrogen bond were used to start the MD-H297(HIE) and MD-H297(HIP) simulations.

**Continuous constant pH molecular dynamics (CpHMD).** We applied the membrane-enabled hybrid-solvent continuous constant pH molecular dynamics (CpHMD) method<sup>22,23</sup> to determine the protonation states of all titratable residues in the mOR systems. In this method, conformational dynamics is propagated in explicit solvent and lipids, while the solvation forces for propagating titration coordinates are calculated using the membrane generalized-Born GBSW model<sup>63</sup> based on the conformations sampled in explicit solvent. To accelerate convergence of the coupled conformational and protonation-state sampling, a replica-exchange protocol in the pH space is used<sup>22</sup>. The membrane-enabled hybrid-solvent CpHMD method<sup>22,23</sup> has been validated for  $pK_a$  calculations and pH-dependent simulations of transmembrane proteins<sup>23,25,26</sup>. The detailed protocols can be found here<sup>24</sup>.

Three sets of replica-exchange CpHMD simulations were performed, starting from the equilibrated apo active mOR structure, equilibrated fentanyl-mOR complex in the D147-binding mode, and the fentanyl-mOR complex in the H297-binding mode obtained from the WE-HID simulation in which the FEN-H297 distance is less than 3.5 Å. The pH replica-exchange protocol included 16 replicas in the pH range 2.5–9.5 with an increment of 0.5 unit. A GB calculation was invoked every 10 MD steps to update the titration coordinates. In the GB calculation, the default settings were used, consistent with our previous work<sup>22</sup>. Each pH replica underwent molecular dynamics in the NPT ensemble with an aggregate sampling time of 320 ns. All Asp, Glu, and His sidechains as well as the piperidine amine were allowed to titrate. The model  $pK_a$ s of Asp, Glu, and His are 3.8, 4.2, and 6.5, respectively<sup>33</sup>, while that of the piperidine amine in fentanyl is 8.9<sup>46</sup>.

**Molecular dynamics protocol.** The temperature and pressure were maintained at 310 K and 1 atm by the Langevin thermostat and Monte Carlo barostat, respectively in the simulations with the Amber program<sup>28</sup>, while the modified Hoover thermostat and Langevin piston coupling method were used in the simulations

with the CHARMM program<sup>56</sup>. Long-range electrostatics was treated by the particle-mesh Ewald (PME) method<sup>64</sup> with a real-space cut-off of 12 Å and a sixth-order interpolation with a 1.6-Å<sup>-1</sup> grid spacing. The van der Waals interactions were smoothly switched to zero between 10 and 12 Å. Bonds involving hydrogen atoms were constrained using the SHAKE algorithm to enable a 2-fs timestep. Analysis was performed using CPPTRAJ program<sup>65</sup>. For analysis of the equilibrium simulations starting from the D147- and H297-binding modes, the last 200 or 400 ns data were used, respectively.

**Clustering analysis.** The clustering analysis was performed using the cluster command in CPPTRAJ<sup>65</sup> with the hierarchical agglomerate algorithm. The distance between clusters was calculated based on the RMSD of fentanyl's heavy atoms. The distance cutoff was 3 Å.

**Calculation of Tanimoto coefficients.** Tanimoto coefficient between profiles A and B is calculated using the following equation:

$$S_{AB} = \frac{\sum_{i=1}^n x_{iA} \cdot x_{iB}}{\sum_{i=1}^n (x_{iA})^2 + \sum_{i=1}^n (x_{iB})^2 - \sum_{i=1}^n x_{iA} \cdot x_{iB}}, \quad (1)$$

where  $x_{iA}$  or  $x_{iB}$  denotes the contact value between fentanyl and residue  $i$  of mOR from profile A or B, respectively.  $x_i$  has a value of 1 if a contact exists and 0 otherwise.

**Binding site volume calculation.** A reviewer noted that BU72 is big and so the second binding mode may be the result of using the BU72-bound mOR crystal structure as a template to generate the initial structure for the fentanyl–mOR complex. The reviewer suggested running a 1-μs MD equilibration of the empty receptor (with the goal to “shrink the binding pocket”). To address this comment, we performed the binding site volume calculations using POVME2.0<sup>66,67</sup>. All structures were first aligned using the Cα atoms of the binding site residues (Tyr75, Gln124, Asn127, Trp133, Ile144, Asp147, Tyr148, Met151, Phe152, Leu232, Lys233, Val236, Ala240, Trp293, Ile296, His297, Val300, Trp318, His319, Ile322, Tyr326) from the BU72-bound mOR crystal structure (PDB ID: 5C1M). All waters, ions, cholesterol, lipids, nanobody, and ligands were removed before the calculation. The binding pocket searching region is kept consistent throughout all systems by specifying an Inclusion box centered at the binding pocket center of mass (0,0,8) and sides of 12 Å, 12 Å, 15 Å in the x, y, and z direction, respectively. For the volume calculation, trajectory snapshots were taken every 5 ns from the last 50 ns of the simulations.

The binding site volume based on the BU72-bound mOR crystal structure (with BU72 removed) is 371 Å<sup>3</sup>. After 110 ns of MD equilibration before docking fentanyl, the volume is 359 ± 12 Å<sup>3</sup>, which is similar to that of the crystal structure. To test if prolonged equilibration would shrink the binding site volume, we extended the simulation by 500 ns and found that the receptor's cavity volume increased to 465 ± 51 Å<sup>3</sup>. An increase in volume can be rationalized as the result of relaxation and solvation of the binding site. Thus, a long MD equilibration of the empty receptor will not reduce the binding site volume, and the alternative binding mode of fentanyl is not a result of an expanded binding cavity due to the size of BU72.

**Reporting summary.** Further information on research design is available in the Nature Research Reporting Summary linked to this article.

## Data availability

Data supporting the findings of this manuscript are available from the corresponding authors upon reasonable request. A reporting summary for this article is available as a Supplementary Information file.

Received: 28 August 2020; Accepted: 8 January 2021;

Published online: 12 February 2021

## References

- CDC WONDER. <https://wonder.cdc.gov/>. (2020).
- Synthetic Opioid Overdose Data. <https://www.cdc.gov/drugoverdose/data/fentanyl.html> (2020).
- Van Bever, W. F., Niemegeers, C. J., Schellekens, K. H. & Janssen, P. A. N-4-Substituted 1-(2-arylethyl)-4-piperidinyl-N-phenylpropanamides, a novel series of extremely potent analgesics with unusually high safety margin. *Arzneimittelforschung*. **26**, 1548–1551 (1976).
- Volpe, D. A. et al. Uniform assessment and ranking of opioid Mu receptor binding constants for selected opioid drugs. *Regul. Toxicol. Pharmacol.* **59**, 385–390 (2011).
- Burns, S. M., Cunningham, C. W. & Mercer, S. L. DARK classics in chemical neuroscience: fentanyl. *ACS Chem. Neurosci.* **9**, 2428–2437 (2018).
- Comer, S. D. & Cahill, C. M. Fentanyl: Receptor pharmacology, abuse potential, and implications for treatment. *Neurosci. Biobehav. Rev.* **106**, 49–57 (2019).
- Vardanyan, R. S. & Hruby, V. J. Fentanyl-related compounds and derivatives: current status and future prospects for pharmaceutical applications. *Future Med. Chem.* **6**, 385–412 (2014).
- Pathan, H. & Williams, J. Basic opioid pharmacology: an update. *Br. J. Pain* **6**, 11–16 (2012).
- Huang, W. et al. Structural insights into μ-opioid receptor activation. *Nature* **524**, 315–321 (2015).
- Manglik, A. Crystal structure of the μ-opioid receptor bound to a morphinan antagonist. *Nature* **485**, 321 (2012).
- Koehl, A. et al. Structure of the μ-opioid receptor-Gi protein complex. *Nature* **558**, 547–552 (2018).
- Ballesteros, J. A. & Weinstein, H. Integrated methods for the construction of three-dimensional models and computational probing of structure-function relations in G protein-coupled receptors. *Methods Neurosci.* **25**, 366–428 (1995).
- Surrat, C. K. et al. Charged transmembrane domain amino acids are critical for agonist recognition and intrinsic activity. *J. Biol. Chem.* **269**, 20548–20553 (1994).
- Mansour, A. et al. Key residues defining the μ-opioid receptor binding pocket: a site-directed mutagenesis study. *J. Neurochem.* **68**, 344–353 (1997).
- Meyer, J., Del Vecchio, G., Seitz, V., Massaly, N. & Stein, C. Modulation of M-opioid receptor activation by acidic pH is dependent on ligand structure and an ionizable amino acid residue. *Br. J. Pharmacol.* **176**, 4510–4520 (2019).
- Ellis, C. R., Kruhlak, N. L., Kim, M. T., Hawkins, E. G. & Stavitskaya, L. Predicting opioid receptor binding affinity of pharmacologically unclassified designer substances using molecular docking. *PLoS ONE* **13**, e0197734 (2018).
- Subramanian, G., Paterlini, M. G., Portoghesi, P. S. & Ferguson, D. M. Molecular docking reveals a novel binding site model for fentanyl at the μ-opioid receptor. *J. Med. Chem.* **43**, 381–391 (2000).
- Lipiński, P. F. J., Jaróńczyk, M., Dobrowski, J. C. & Sadlej, J. Molecular dynamics of fentanyl bound to μ-opioid receptor. *J. Mol. Model.* **25**, 144 (2019).
- Huber, G. & Kim, S. Weighted-ensemble Brownian dynamics simulations for protein association reactions. *Biophys. J.* **70**, 97–110 (1996).
- Zwier, M. C. et al. WESTPA: an interoperable, highly scalable software package for weighted ensemble simulation and analysis. *J. Chem. Theory Comput.* **11**, 800–809 (2015).
- Zuckerman, D. M. & Chong, L. T. Weighted ensemble simulation: review of methodology, applications, and software. *Annu. Rev. Biophys.* **46**, 43–57 (2017).
- Wallace, J. A. & Shen, J. K. Continuous constant pH molecular dynamics in explicit solvent with pH-based replica exchange. *J. Chem. Theory Comput.* **7**, 2617–2629 (2011).
- Huang, Y., Chen, W., Dotson, D. L., Beckstein, O. & Shen, J. Mechanism of pH-dependent activation of the sodium-proton antiporter NhaA. *Nat. Commun.* **7**, 12940 (2016).
- Huang, Y., Henderson, J. A. & Shen, J. Continuous constant pH molecular dynamics simulations of transmembrane proteins. *Methods Mol. Biol.* in press (2020).
- Chen, W., Huang, Y. & Shen, J. Conformational activation of a transmembrane proton channel from constant pH molecular dynamics. *J. Phys. Chem. Lett.* **7**, 3961–3966 (2016).
- Yue, Z., Chen, W., Zgurskaya, H. I. & Shen, J. Constant pH molecular dynamics reveals how proton release drives the conformational transition of a transmembrane efflux pump. *J. Chem. Theory Comput.* **13**, 6405–6414 (2017).
- Henderson, J. A., Huang, Y., Beckstein, O. & Shen, J. Alternative proton-binding site and long-distance coupling in *Escherichia coli* sodium–proton antiporter NhaA. *Proc. Natl. Acad. Sci. USA* **117**, 25517–25522 (2020).
- Case, D. A. et al. AMBER 2018, University of California, San Francisco <https://ambermd.org/doc12/Amber18.pdf> (2018).
- Yuan, S., Vogel, H. & Filipek, S. The role of water and sodium ions in the activation of the μ-opioid receptor. *Angew. Chem. Int. Ed.* **52**, 10112–10115 (2013).
- Katritch, V. et al. Allosteric sodium in class A GPCR signaling. *Trends Biochem. Sci.* **39**, 233–244 (2014).
- Cong, X. et al. Structural determinants for the binding of morphinan agonists to the μ-Opioid Receptor. *PLoS ONE* **10**, e0135998 (2015).
- Schneider, S., Provasi, D. & Filizola, M. How oliceridine (TRV-130) binds and stabilizes a μ-opioid receptor conformational state that selectively triggers G protein signaling pathways. *Biochemistry* **55**, 6456–6466 (2016).
- Thurkill, R. L., Grimsley, G. R., Scholtz, J. M. & Pace, C. N. P.K values of the ionizable groups of proteins. *Protein Sci.* **15**, 1214–1218 (2006).
- Maguire, P., Tsai, N., Cometta-Morini, C. & Loew, G. Pharmacological profiles of fentanyl analogs at Mu, Delta and Kappa opiate receptors. *Eur. J. Pharmacol.* **213**, 219–225 (1992).

35. Casy, A. F. & Huckstep, M. R. Structure-activity studies of fentanyl. *J. Pharm. Pharmacol.* **40**, 605–608 (1988).
36. Lipiński, P. F. J. et al. Fentanyl family at the Mu-opioid receptor: uniform assessment of binding and computational analysis. *Molecules* **24**, 740 (2019).
37. Willett, P., Barnard, J. M. & Downs, G. M. Chemical similarity searching. *J. Chem. Inf. Comput. Sci.* **38**, 983–996 (1998).
38. Chaturvedi, K., Shahrestanifar, M. & Howells, R. D.  $\mu$  Opioid receptor: role for the amino terminus as a determinant of ligand binding affinity. *Mol. Brain Res.* **76**, 64–72 (2000).
39. United Nations Office on Drugs and Crime. *Fentanyl and its analogues—50 Years On* (Global Smart Update, United Nations Office on Drugs and Crime, 2017).
40. Debiec, K. T. et al. Further along the road less traveled: AMBER ff15ipq, an original protein force field built on a self-consistent physical model. *J. Chem. Theory Comput.* **12**, 3926–3947 (2016).
41. Best, R. B. et al. Optimization of the additive CHARMM all-atom protein force field targeting improved sampling of the backbone  $\phi$ ,  $\psi$  and side-chain  $\chi_1$  and  $\chi_2$  dihedral angles. *J. Chem. Theory Comput.* **8**, 3257–3273 (2012).
42. Huang, J. et al. CHARMM36m: an improved force field for folded and intrinsically disordered proteins. *Nat. Methods* **14**, 71–73 (2017).
43. Suárez, E. et al. Simultaneous computation of dynamical and equilibrium information using a weighted ensemble of trajectories. *J. Chem. Theory Comput.* **10**, 2658–2667 (2014).
44. Spahn, V. et al. A nontoxic pain killer designed by modeling of pathological receptor conformations. *Science* **355**, 966–969 (2017).
45. Spahn, V. et al. Opioid receptor signaling, analgesic and side effects induced by a computationally designed pH-dependent agonist. *Sci. Rep.* **8**, 8965 (2018).
46. Roy, S. D. & Flynn, G. L. Solubility behavior of narcotic analgesics in aqueous media: solubilities and dissociation constants of morphine, fentanyl, and sufentanil. *Pharm. Res.* **6**, 147–151 (1989).
47. Thurlkill, R. L., Cross, D. A., Scholtz, J. M. & Pace, C. N. pKa of fentanyl varies with temperature: implications for acid-base management during extremes of body temperature. *J. Cardiothorac. Vasc. Anesth.* **19**, 759–762 (2005).
48. Rosas, R., Huang, X.-P., Roth, B. L. & Dockendorff, C.  $\beta$ -fluorofentanyl are pH-sensitive Mu opioid receptor agonists. *ACS Med. Chem. Lett.* **10**, 1353–1356 (2019).
49. Chan, H. C. S. et al. Exploring a new ligand binding site of G protein-coupled receptors. *Chem. Sci.* **9**, 6480–6489 (2018).
50. Vickery, O. N. et al. Intracellular transfer of Na<sup>+</sup> in an active-state G-protein-coupled receptor. *Structure* **26**, 171–180.e2 (2018).
51. Alexov, E. et al. Progress in the prediction of pKa values in proteins. *Proteins* **79**, 3260–3275 (2011).
52. Lee, J. et al. CHARMM-GUI input generator for NAMD, GROMACS, AMBER, OpenMM, and CHARMM/OpenMM simulations using the CHARMM36 additive force field. *J. Chem. Theory Comput.* **12**, 405–413 (2016).
53. Huang, Y., Chen, W., Wallace, J. A. & Shen, J. All-atom continuous constant pH molecular dynamics with particle mesh Ewald and titratable water. *J. Chem. Theory Comput.* **12**, 5411–5421 (2016).
54. Zwier, M. C., Kaus, J. W. & Chong, L. T. Efficient explicit-solvent molecular dynamics simulations of molecular association kinetics: methane/methane, Na<sup>+</sup>/Cl<sup>-</sup>, Methane/Benzene, and K<sup>+</sup>/18-Crown-6 Ether. *J. Chem. Theory Comput.* **7**, 1189–1197 (2011).
55. Vilardaga, J.-P., Bünenmann, M., Krasel, C., Castro, M. & Lohse, M. J. Measurement of the millisecond activation switch of G protein-coupled receptors in living cells. *Nat. Biotechnol.* **21**, 807–812 (2003).
56. Brooks, B. R. et al. CHARMM: The biomolecular simulation program. *J. Comput. Chem.* **30**, 1545–1614 (2009).
57. MacKerell, Jr., A. D. et al. All-atom empirical potential for molecular modeling and dynamics studies of proteins. *J. Phys. Chem. B* **102**, 3586–3616 (1998).
58. MacKerell, Jr., A. D., Feig, M. & Brooks, I. I. I., C. L. Extending the treatment of backbone energetics in protein force fields: limitations of gas-phase quantum mechanics in reproducing protein conformational distributions in molecular dynamics simulations. *J. Comput. Chem.* **25**, 1400–1415 (2004).
59. Klauda, J. B. et al. Update of the CHARMM all-atom additive force field for lipids: validation on six lipid types. *J. Phys. Chem. B* **114**, 7830–7843 (2010).
60. Vanommeslaeghe, K., Raman, E. P. & MacKerell, A. D. Automation of the CHARMM general force field (CGenFF) II: assignment of bonded parameters and partial atomic charges. *J. Chem. Inf. Model.* **52**, 3155–3168 (2012).
61. Zhang, L. & Hermans, J. Hydrophilicity of cavities in proteins. *Proteins* **24**, 433 (1996).
62. Lomize, M. A., Pogozheva, I. D., Joo, H., Mosberg, H. I. & Lomize, A. L. OPM database and PPM web server: Resources for positioning of proteins in membranes. *Nucleic Acids Res.* **40**, D370–D376 (2012).
63. Im, W., Feig, M. & Brooks, C. L. An implicit membrane generalized born theory for the study of structure, stability, and interactions of membrane proteins. *Biophys. J.* **85**, 2900–2918 (2003).
64. Darden, T., York, D. & Pedersen, L. Particle mesh Ewald: An  $N \cdot \log(N)$  method for Ewald sums in large systems. *J. Chem. Phys.* **98**, 10089–10092 (1993).
65. Roe, D. R. & Cheatham, T. E. PTRAJ and CPPTRAJ: software for processing and analysis of molecular dynamics trajectory data. *J. Chem. Theory Comput.* **9**, 3084–3095 (2013).
66. Durrant, J. D., de Oliveira, C. A. F. & McCammon, J. A. POVME: an algorithm for measuring binding-pocket volumes. *J. Mol. Graph. Model.* **29**, 773–776 (2011).
67. Durrant, J. D., Votapka, L., Sørensen, J. & Amaro, R. E. POVME 2.0: an enhanced tool for determining pocket shape and volume characteristics. *J. Chem. Theory Comput.* **10**, 5047–5056 (2014).

## Acknowledgements

The authors acknowledge financial support from FDA's Safety Research Interest Group and appointment to the Research Participation Programs at the Oak Ridge Institute for Science and Education through an interagency agreement between the Department of Energy and FDA. Financial support from the National Institutes of Health (GM098818) to J.S. and P.M. is also acknowledged.

## Author contributions

J.S. and C.R.E. designed the research. Q.N.V. performed the simulations with the help of P.M. Q.N.V., P.M., J.S., and C.R.E. analyzed the data. Q.N.V., J.S., and C.R.E. wrote the manuscript.

## Competing interests

The authors declare no competing interests.

## Additional information

**Supplementary information** The online version contains supplementary material available at <https://doi.org/10.1038/s41467-021-21262-9>.

**Correspondence** and requests for materials should be addressed to J.S. or C.R.E.

**Peer review information** *Nature Communications* thanks Alissa Hummer and the other, anonymous, reviewer(s) for their contribution to the peer review of this work. Peer reviewer reports are available.

**Reprints and permission information** is available at <http://www.nature.com/reprints>

**Publisher's note** Springer Nature remains neutral with regard to jurisdictional claims in published maps and institutional affiliations.



**Open Access** This article is licensed under a Creative Commons Attribution 4.0 International License, which permits use, sharing, adaptation, distribution and reproduction in any medium or format, as long as you give appropriate credit to the original author(s) and the source, provide a link to the Creative Commons license, and indicate if changes were made. The images or other third party material in this article are included in the article's Creative Commons license, unless indicated otherwise in a credit line to the material. If material is not included in the article's Creative Commons license and your intended use is not permitted by statutory regulation or exceeds the permitted use, you will need to obtain permission directly from the copyright holder. To view a copy of this license, visit <http://creativecommons.org/licenses/by/4.0/>.

© The Author(s) 2021

# **Supplementary Information:**

## **How $\mu$ -Opioid Receptor Recognizes Fentanyl**

Quynh N. Vo,<sup>†,‡</sup> Paween Mahinthichaichan,<sup>‡</sup> Jana Shen,<sup>\*,‡</sup> and  
Christopher R. Ellis<sup>\*,†</sup>

<sup>†</sup> *Center for Drug Evaluation and Research, United State Food and Drug Administration,  
Silver Spring, Maryland 20993, United States*

<sup>‡</sup> *Department of Pharmaceutical Science, University of Maryland School of Pharmacy,  
Baltimore, Maryland 21201, United States*

E-mail: jana.shen@rx.umaryland.edu; christopher.ross.ellis@gmail.com

## List of Supplementary Tables

1	Simulation steps for apo active mOR . . . . .	3
2	Simulation steps to relax the docked structure . . . . .	3
3	Simulation steps to relax the H297 binding mode . . . . .	4
4	Calculated $pK_a$ 's of mOR and fentanyl . . . . .	4

## List of Supplementary Figures

1	Equilibration of the docked fentanyl-mOR structure . . . . .	5
2	Fentanyl position in the WE-HIE simulation . . . . .	6
3	Fentanyl position in the WE-HID simulation . . . . .	7
4	The $pK_a$ of His297 is converged in the replica-exchange CpHMD simulations	8
5	The D147 salt bridge is stable regardless of His297's protonation state . . .	9
6	Aromatic stacking between fentanyl's phenethyl group and Trp293 of mOR .	10
7	Occupancies of the intra- and intermolecular hydrogen bonds . . . . .	11
8	Fentanyl is pushed away from HIE297 or HIP297 . . . . .	12
9	Trp293 $\chi_2$ angle is different from the BU72-bound mOR structure . . . . .	13
10	Fentanyl adopts different orientations in the two binding modes . . . . .	14
11	His297's $\chi_2$ angle is influenced by the protonation state . . . . .	15
12	Characterization of the equilibrium simulations . . . . .	16
13	Comparison between fentanyl-mOR contacts and BU72-, DAMGO-, or $\beta$ -FNA contacts with mOR . . . . .	17

## Supplementary Tables

**Supplementary Table 1** Steps in the equilibration simulation of apo active mOR

Step	Ensemble	Time (ns)	BB <sup>a</sup>	mOR Wat <sup>a</sup>	Lipid <sup>b</sup>
1	NVT	0.35	10.0	5.00	5.0 / 2500
2	NVT	0.15	5.00	2.50	5.0 / 200
3	NPT	0.50	5.00	2.50	5.0 / 200
4	NPT	0.50	2.50	1.25	2.0 / 100
5	NPT	1.00	2.50	1.25	1.0 / 100
6	NPT	1.00	2.50	1.25	0.5 / 50
7	NPT	4.00	2.50	1.25	0
8	NPT	60.0	2.50	1.25	0
9	NPT	50.0	0	0	0

<sup>a</sup> Force constant in the harmonic restraint potential for the backbone heavy atoms in kcal/mol/Å<sup>2</sup>. <sup>b</sup> Force constant in the position/dihedral restraint potential. The unit is kcal/mol/Å<sup>2</sup> for the position restraints or kcal/mol for dihedral angle restraints. mOR Wat refers to the crystal waters and seven additional water added using the program DOWSER.<sup>1</sup>

**Supplementary Table 2** Steps in the equilibration simulation to relax the docked fentanyl-mOR complex structure

Step	Ensemble	Time (ns)	BB <sup>a</sup>	SC <sup>a</sup>	fentanyl <sup>b</sup>
1	NPT	1.00	2.50	1.25	2.50
2	NPT	1.00	1.25	0.75	1.25
3	NPT	1.00	1.00	0.50	1.00
4	NPT	1.00	0.50	0.25	0.50
5	NPT	1.00	0.25	0	0.25
6	NPT	110.0	0	0	0

<sup>a</sup> Force constant in the harmonic restraint potential for the backbone and sidechain heavy atoms in kcal/mol/Å<sup>2</sup>. <sup>b</sup> Force constant in the harmonic restraint potential for the fentanyl heavy atoms.

**Supplementary Table 3** Steps in the equilibration simulation to relax the H297 binding mode with H297 as either HIE or HIP

Step	Ensemble	Time (ns)	BB <sup>a</sup>	SC <sup>a</sup>	fentanyl <sup>b</sup>
1	NPT	1.00	2.50	1.25	2.50
2	NPT	1.00	1.25	0.75	1.25
3	NPT	1.00	1.00	0.50	1.00
4	NPT	1.00	0.50	0.25	0.50
5	NPT	1.00	0.25	0	0.25
6	NPT	60.0	0	0	0

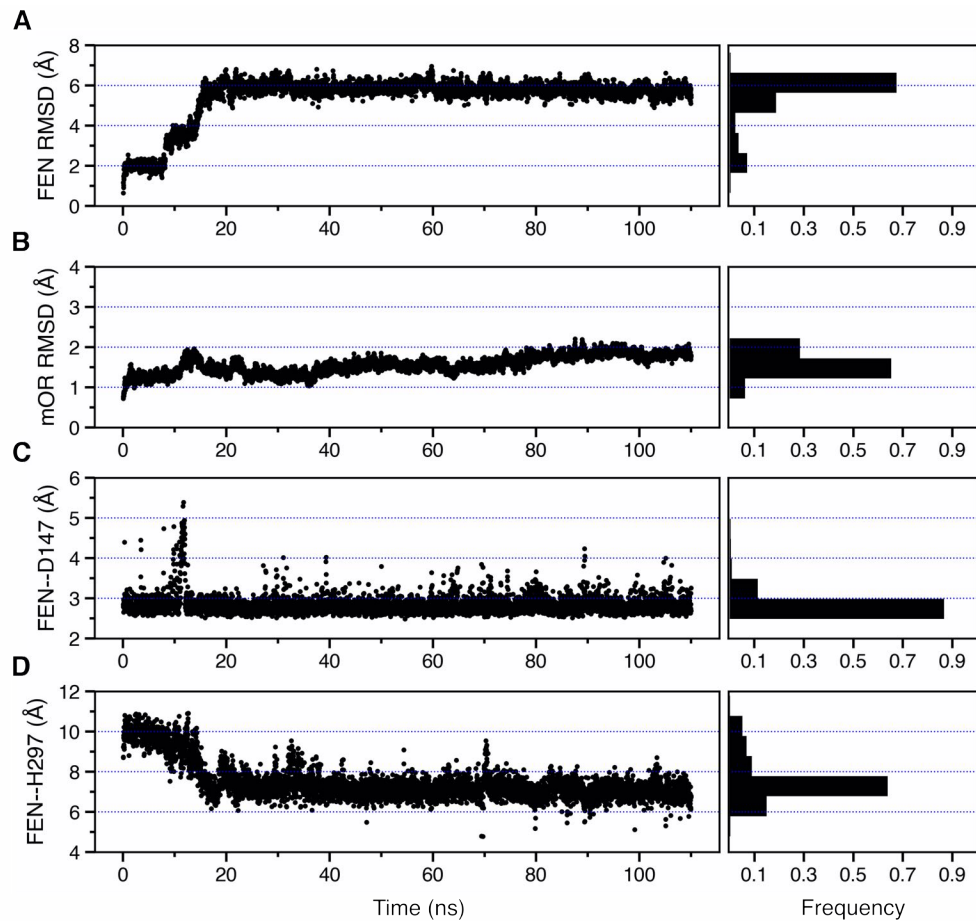
<sup>a</sup> Force constant in the harmonic restraint potential for the backbone and sidechain heavy atoms in kcal/mol/Å<sup>2</sup>. <sup>b</sup> Force constant in the harmonic restraint potential for the fentanyl heavy atoms.

**Supplementary Table 4** Calculated pK<sub>a</sub>'s of mOR titratable residues and fentanyl from the pH replica-exchange CpHMD simulations

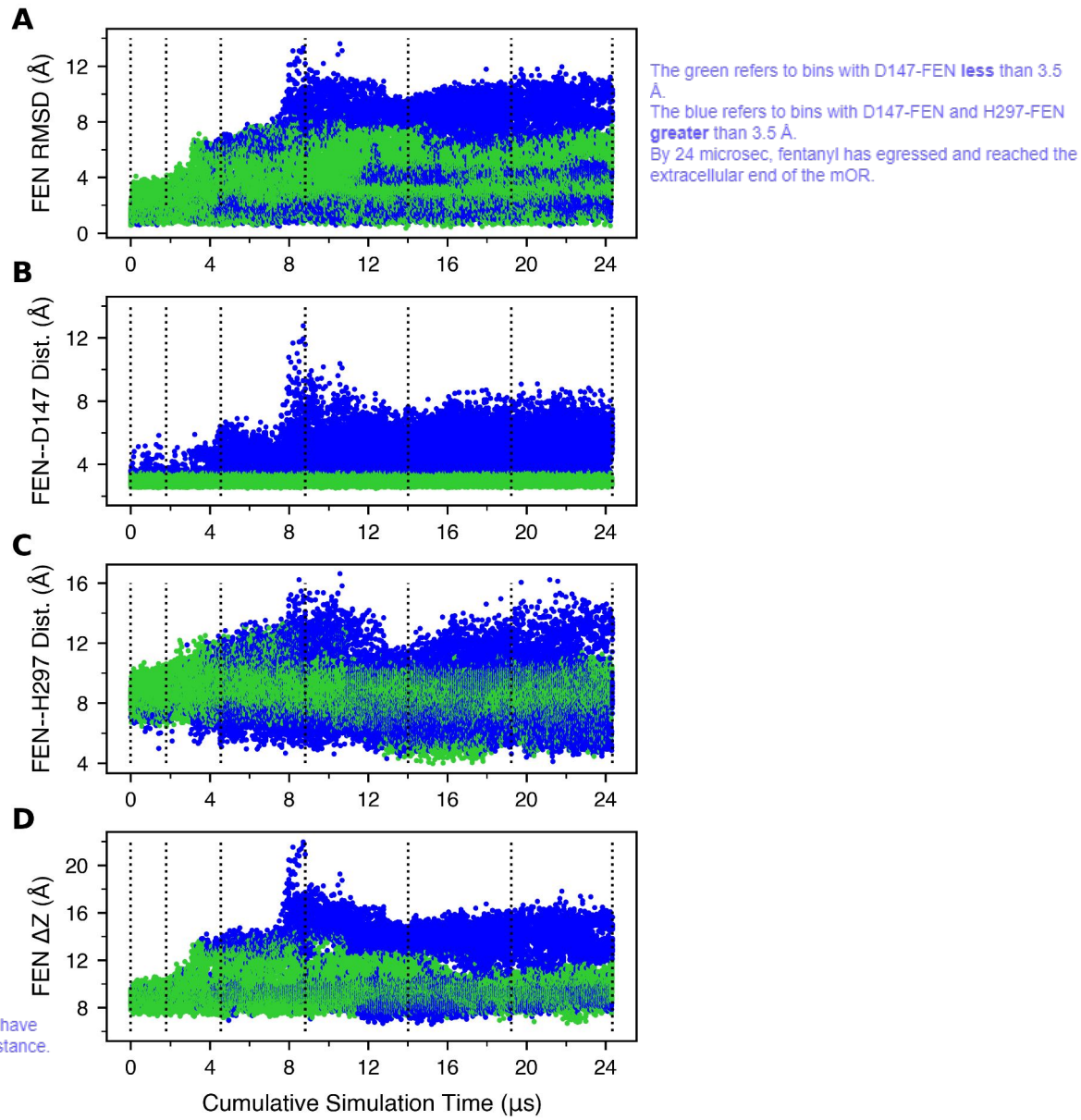
Residue	CpH-apo	CpH-D147	CpH-H297
Asp114	4.8	5.1	4.8
Asp147	3.3	4.1	3.8
Asp164	3.6	2.8	3.0
Asp177	3.6	3.8	3.8
Asp216	2.5	2.9	2.5
Asp272	2.6	2.0	1.9
Asp340	3.3	3.3	3.2
Glu229	3.2	2.8	2.9
Glu270	3.5	3.3	3.3
Glu310	3.8	3.2	3.7
Glu341	3.2	3.5	3.0
His54	6.8	7.3	7.5
His171	5.6	5.3	5.2
His223	5.8	5.8	5.7
His297	6.8	7.3	6.7
His319	7.1	7.2	6.8
Fentanyl	NA	>9.5 <sup>a</sup>	>9.5 <sup>a</sup>

<sup>a</sup> Only a lower bound to the pK<sub>a</sub> of the piperidine amine of fentanyl is given, as the amine remains charged in the entire simulation pH range 2.5–9.5.

## Supplementary Figures

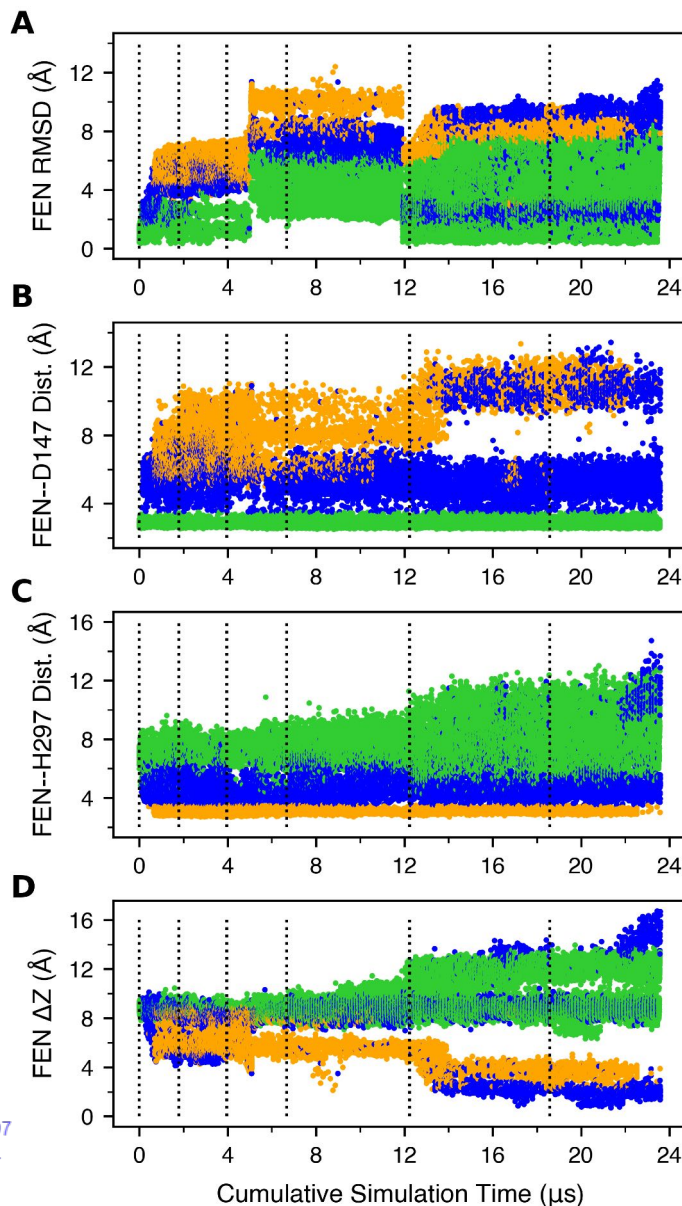


**Supplementary Fig. 1 Equilibration of the docked fentanyl-mOR structure. A, B.** Time series of the root-mean-square deviation (RMSD) of the fentanyl (A) and mOR (B) heavy atom positions with respect to their starting positions. **C.** Time series of the FEN–D147 distance, defined as the minimum distance between the piperidine nitrogen and the carboxylate oxygen of Asp147. **D.** Time series of the FEN–H297 distance, defined as that between the piperidine nitrogen and the unprotonated imidazole nitrogen of His297.



**Supplementary Fig. 2 Fentanyl position as a function of the cumulative simulation time of the WE-HIE simulation.** **A.** The root-mean-square deviation (RMSD) of the fentanyl heavy atoms with respect to the starting position. **B.** The FEN–D147 distance refers to the minimum distance between the piperidine nitrogen and the carboxylate oxygen of Asp147. **C.** The FEN–H297 distance is measured between the piperidine nitrogen and the unprotonated imidazole nitrogen of His297. **D.** Fentanyl  $\Delta Z$  position is defined as the distance between the centers of mass (COM) of fentanyl and mOR in the z direction. Data with the FEN–D147 and FEN–H297 distances below 3.5  $\text{\AA}$  are colored green and orange, respectively, and otherwise blue. The unweighted data from all bins were taken and the time refers to the cumulative time. the vertical lines are drawn at every 50 weighted ensemble iterations.

The green refers to bins with D147-FEN **less** than 3.5 Å.  
The orange refers to bins with H297-FEN **less** than 3.5 Å.  
The blue refers to bins with D147-FEN and H297-FEN **greater** than 3.5 Å.  
By 24 microsec, fentanyl has egressed and reached the extracellular end of the mOR.



Definitely important to point out that HID has H297 interaction less than 3.5 hydrogen bond distance.

a. general make sense that as with the hydrogen bonding with the 2 critical residues, the RMSD is lower because hydrogen bonds stabilizes the ligand. If the distance between ligand and the two critical residue increases, then it means its dissociating from the pocket.

b. makes sense why there is a blob of green at the bottom. bc green means less than 3.5. Orange and blue are greater than 3.5.

c. makes sense orange is a blob at the bottom. this indicate that it is less than 3.5 both green and blue can have greater than 3 fen-H297 distance

d. Super different than in SI Fig2. Blue seems to be overlapping into orange and green regions. Although there is a distinct difference between the green zones and orange zones.

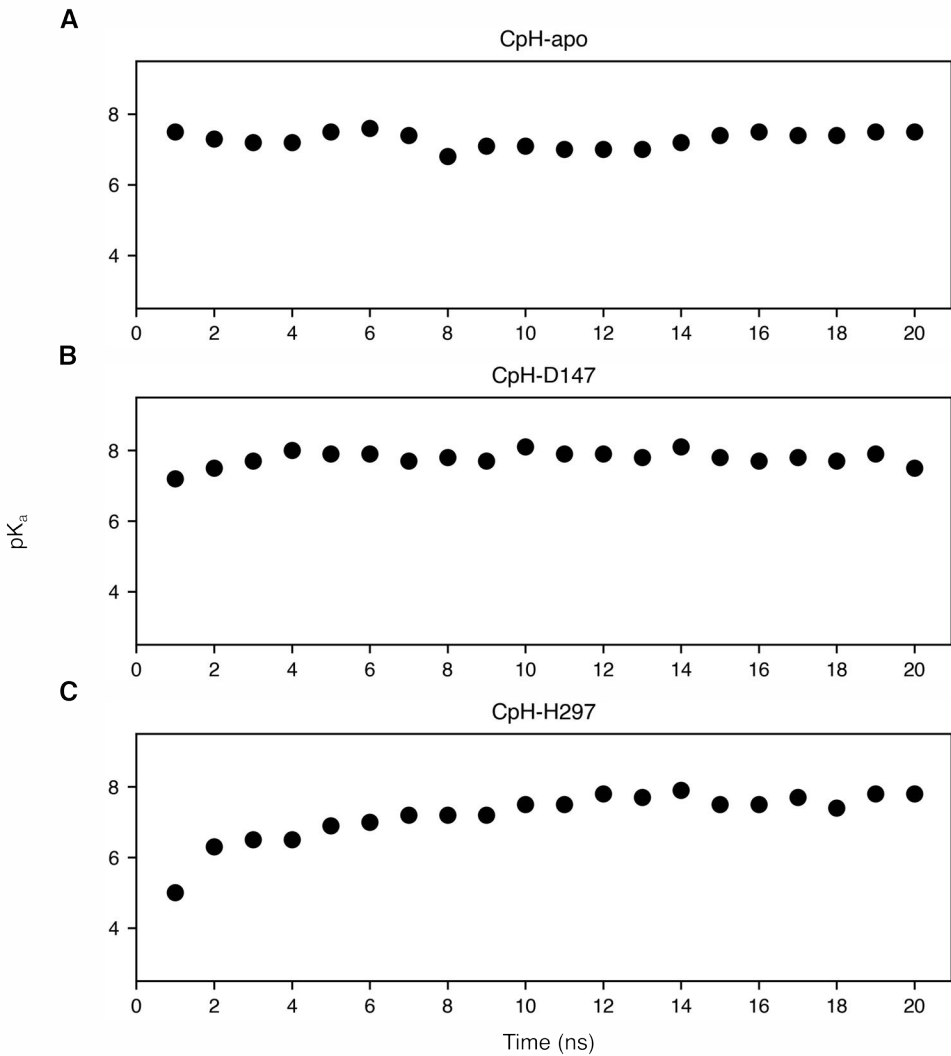
Based on the paper, fentanyl did not egress in the HID297 config. Instead it is sampling the D147 and HID297 bond configuration along with positions in which it does not interact with either residue.

#### Connecting between A & D

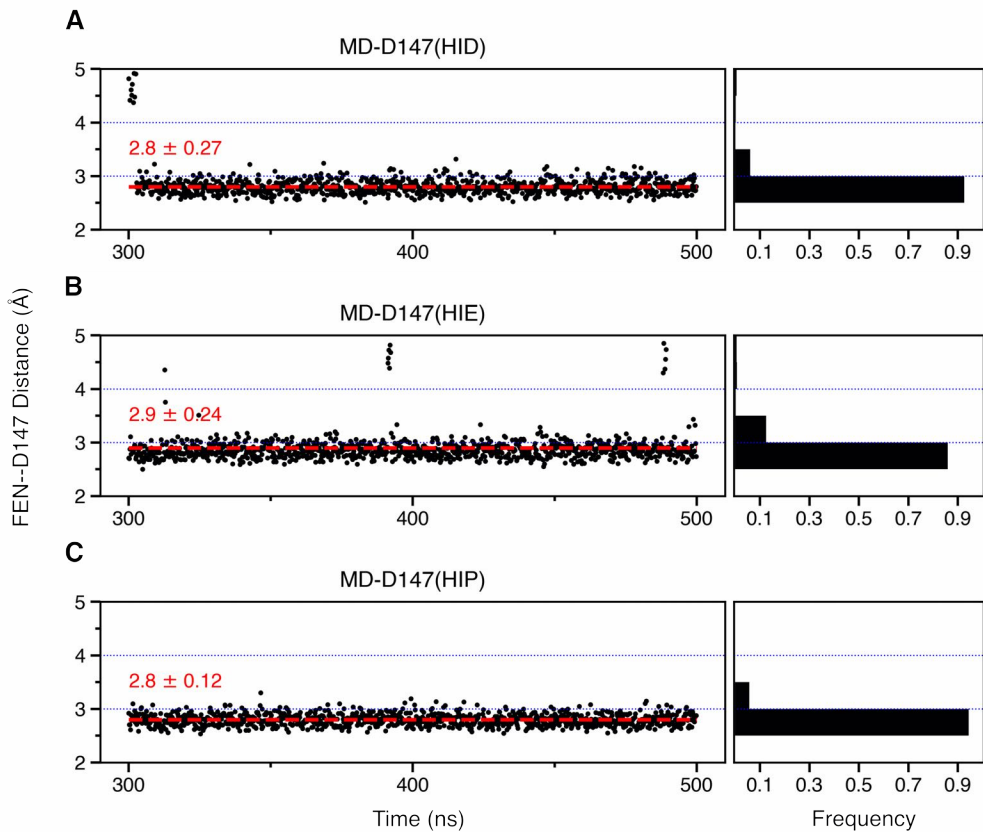
IT MAKES TOTAL SENSE, because the starting conformation is D147 salt bridge position so of course there will be a large RMSD for orange because large conformational change by 0.6 microsec.

In the intro, it says FEN makes significant interactions with the binding pocket when it interacts with H297 than with D147. There is less RMSD fluctuation in orange than green after you disregard the 0.6 when it's finding the HIS salt bridge spot.

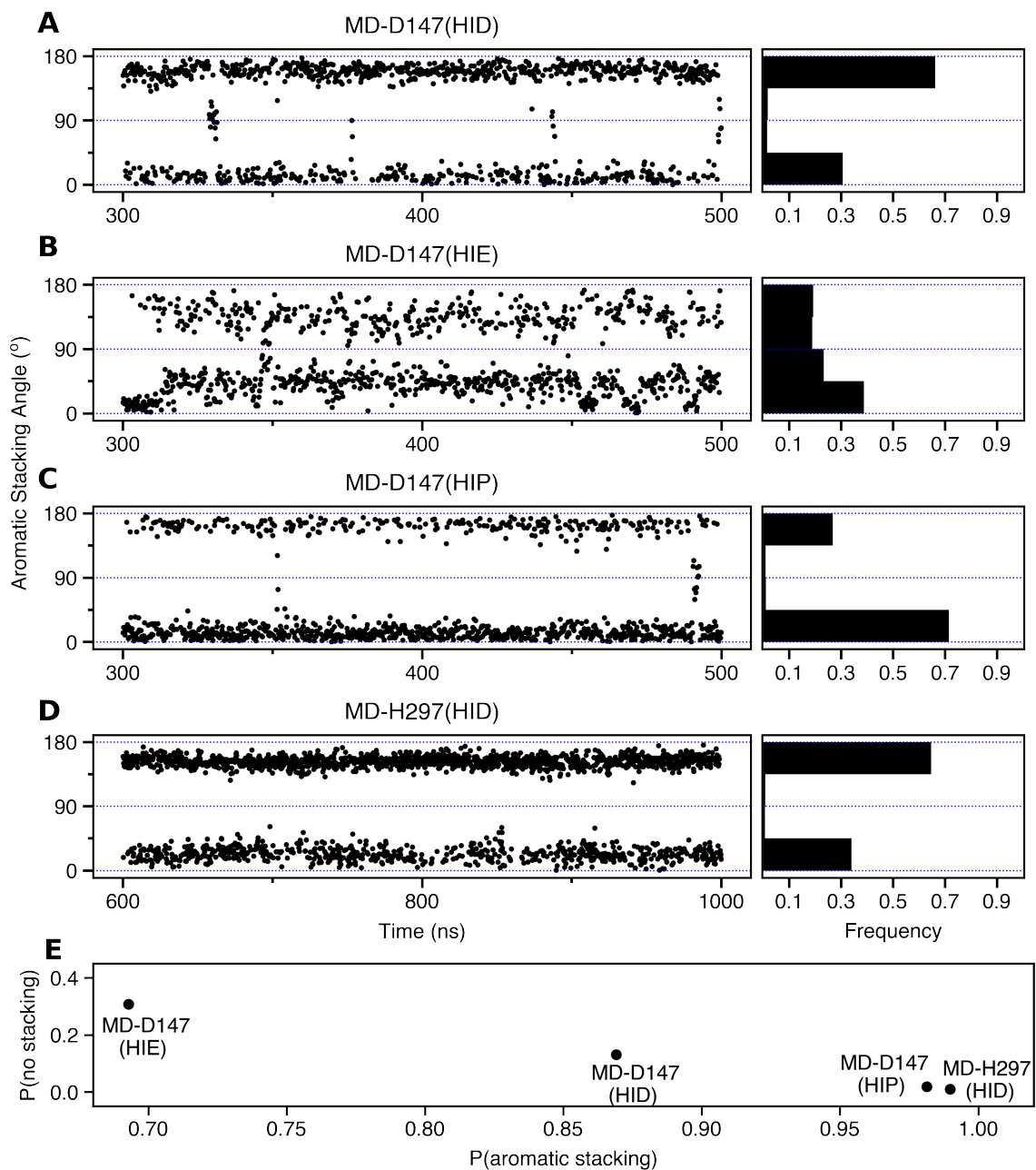
**Supplementary Fig. 3 Fentanyl position as a function of the cumulative simulation time of the WE-HID simulation.** **A.** The root-mean-square deviation (RMSD) of the fentanyl heavy atoms. An abrupt change near  $\sim 5 \mu\text{s}$  is due to the manual bin boundary modification and does not affect the sampling results. **B.** The FEN–D147 distance refers to the minimum distance between the piperidine nitrogen and the carboxylate oxygen of Asp147. **C.** The FEN–H297 distance is measured between the piperidine nitrogen and the unprotonated imidazole nitrogen of His297. **D.** Fentanyl  $\Delta Z$  position is defined as the distance between the centers of mass (COM) of fentanyl and mOR in the z direction. Data with the FEN–D147 and FEN–H297 distances below 3.5 Å are colored green and orange, respectively, and otherwise blue. The unweighted data from all bins were taken and the time refers to the cumulative time. the vertical lines are drawn at every 50 weighted ensemble iterations.



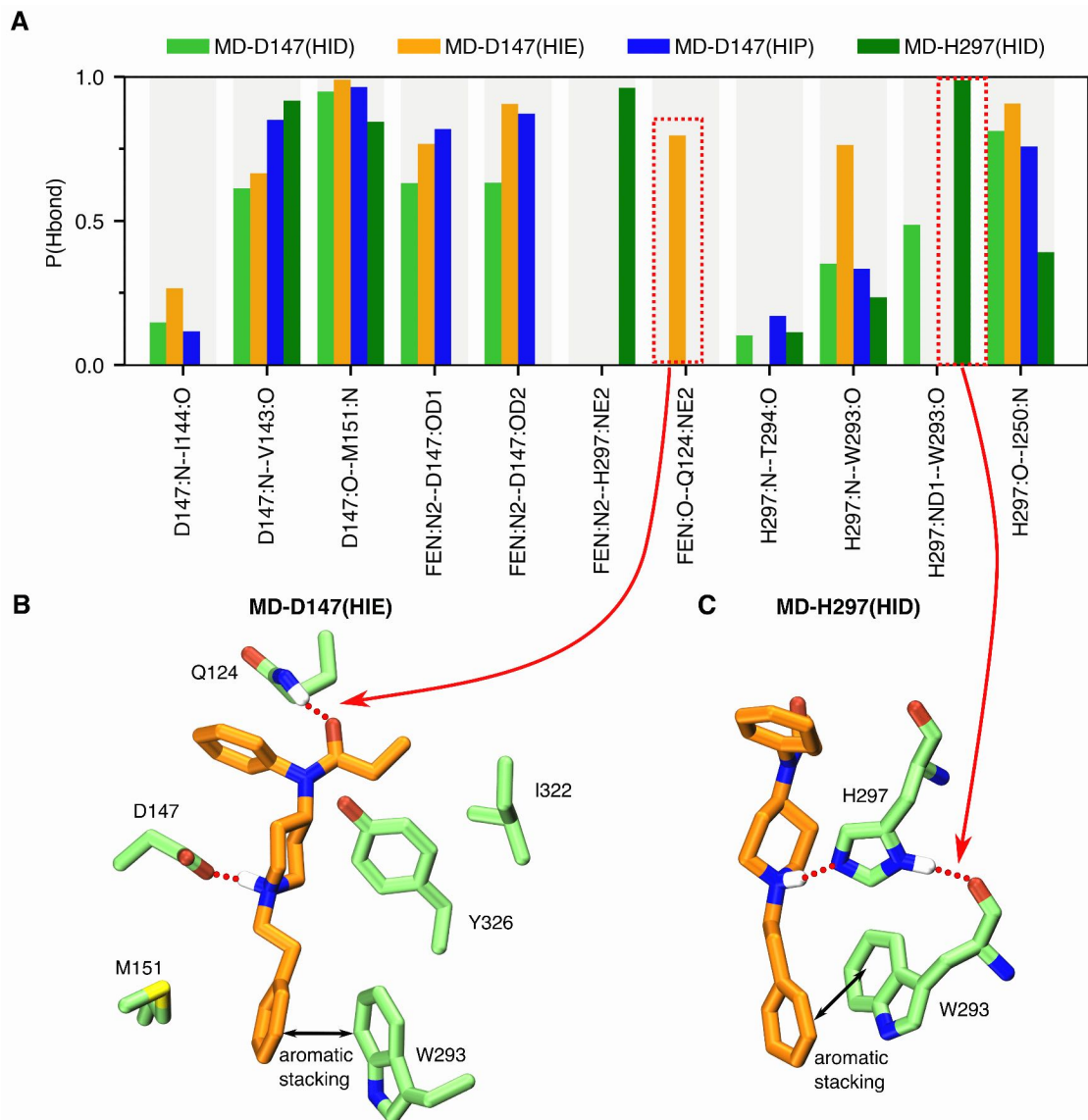
**Supplementary Fig. 4 The  $pK_a$  of His297 is converged in all three sets of replica-exchange CpHMD simulations.** The  $pK_a$  value of His297 plotted every 1-ns as a function of the single replica sampling time from the CpH-apo (**A**), CpH-D147 (**B**), and CpH-H297 (**C**) simulations.



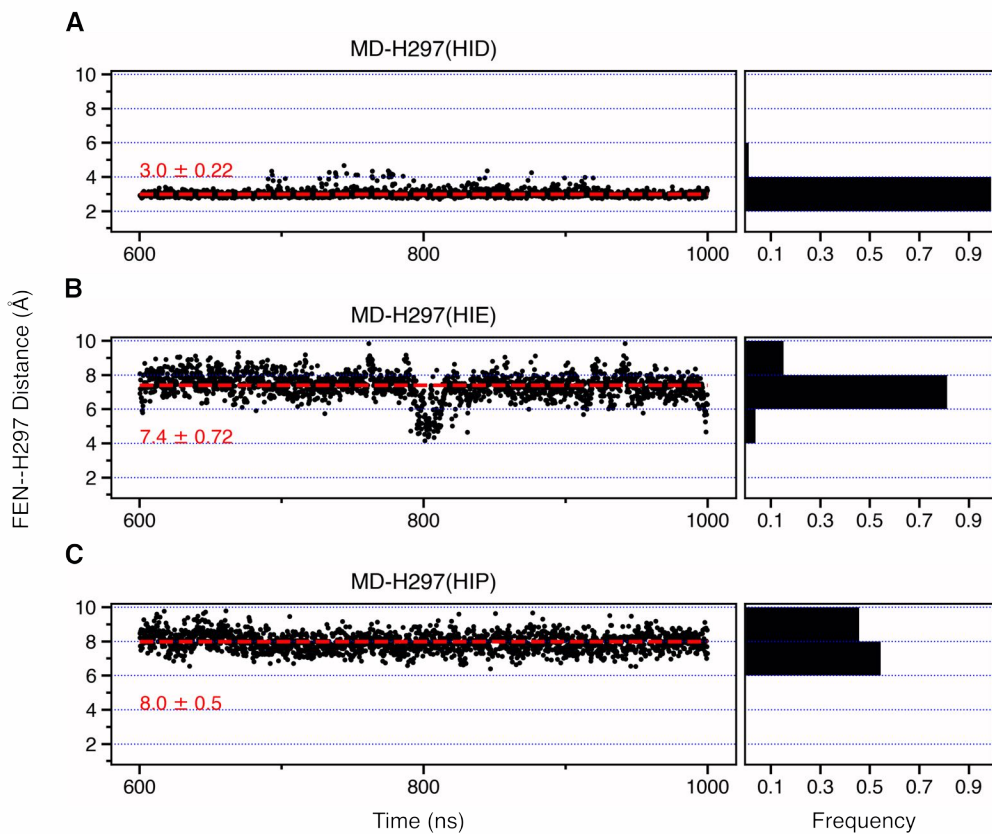
**Supplementary Fig. 5 The D147 salt bridge is stable regardless of the His297 protonation state in the equilibrium simulations of the D147-binding mode.** The time series of the FEN–D147 distance in the presence of HID297 (**A**), HIE297 (**B**) , and HIP297 (**C**) in the equilibrium simulations of the D147-binding mode. The FEN–D147 distance refers to the minimum distance between the piperidine nitrogen and the carboxylate oxygen of Asp147.



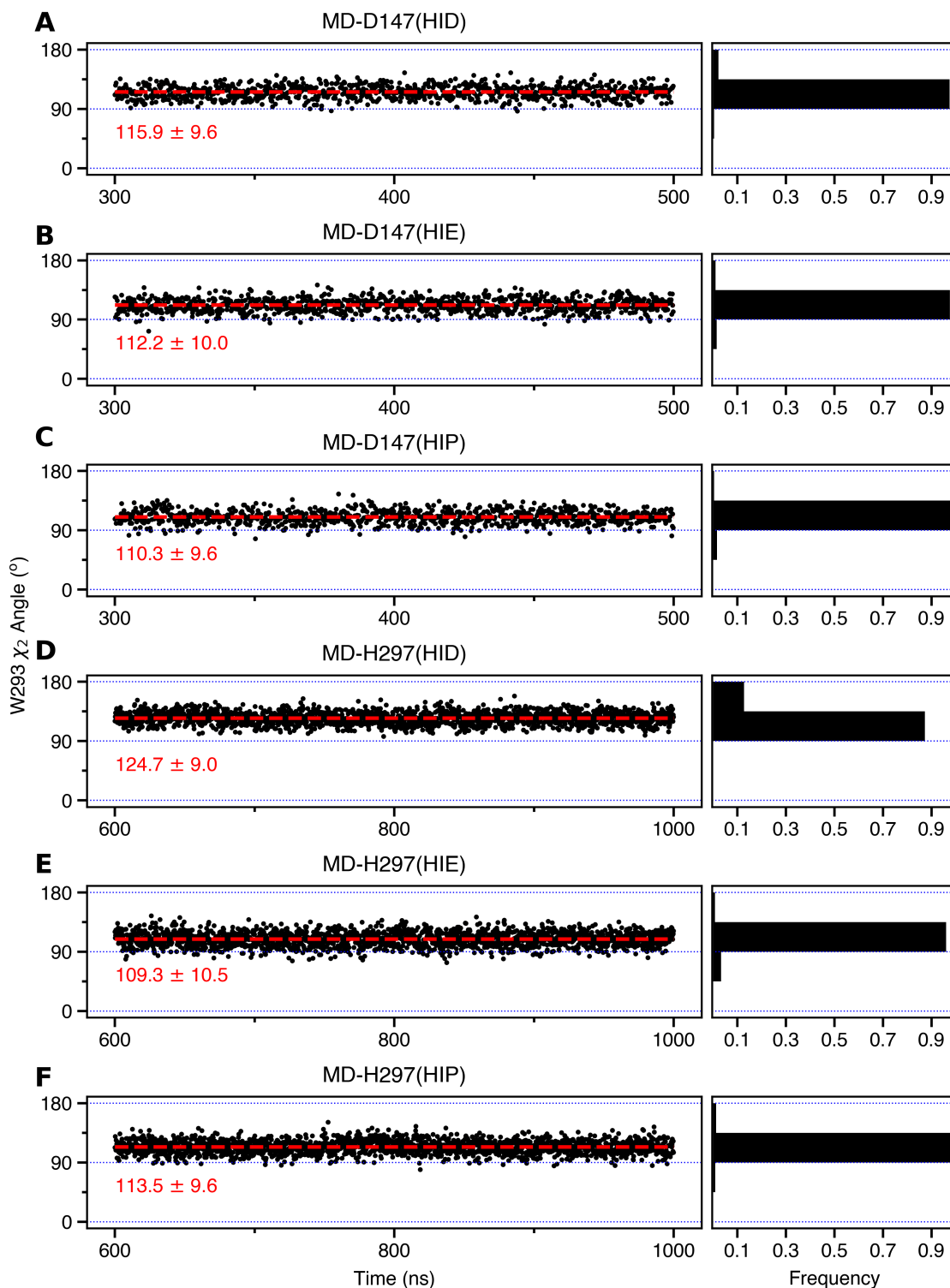
**Supplementary Fig. 6 Aromatic stacking interaction between the phenyl ring of fentanyl's phenethyl group and Trp293 is persistent for both D147- and H297-binding modes.** Time series of the fentanyl-W293 stacking angle from the D147-binding-mode simulations with HID297 (**A**), HIE297 (**B**), or HIP297 (**C**), and from the H297-binding-mode simulation with HID297 (**D**). **E.** Relationship between the probabilities of aromatic stacking and no aromatic stacking from each simulation. The angle is measured between the planes of the phenyl ring of fentanyl's phenethyl group and the six-member ring of Trp293. There is aromatic stacking interaction if the angle between the two planes is within 0–45° or 135–180°.



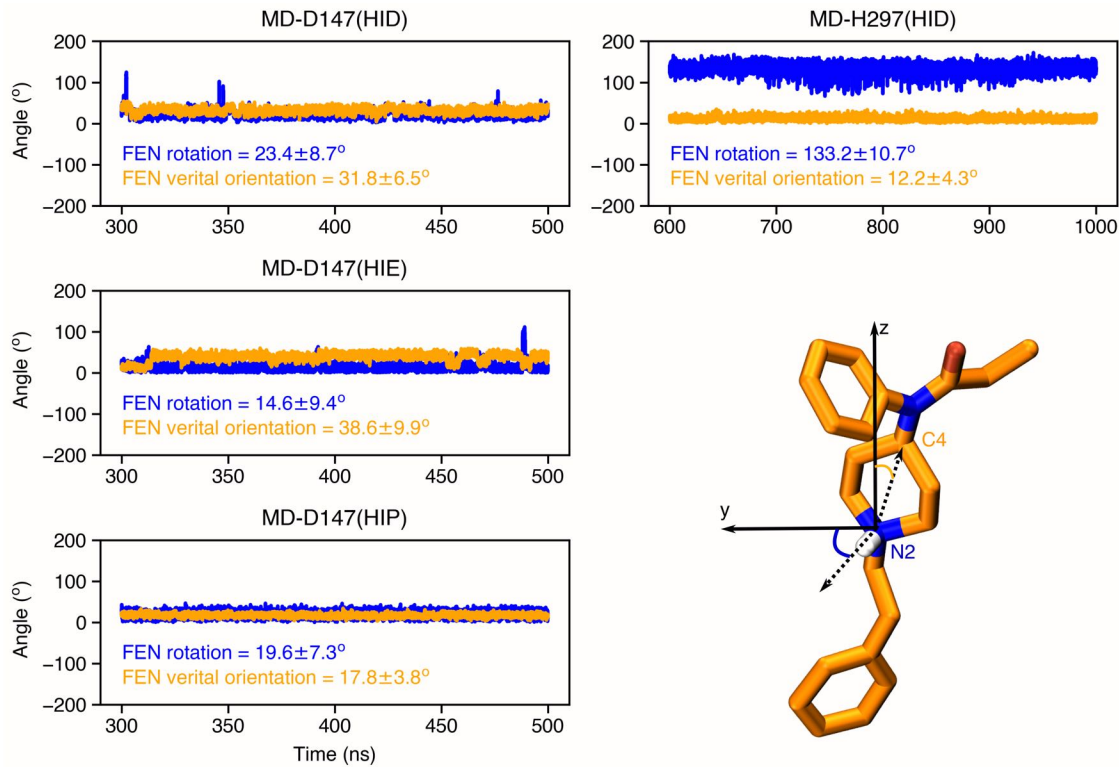
**Supplementary Fig. 7 Occupancies of the intra- and intermolecular hydrogen bonds from the simulations of the D147- and H297-binding modes.** The bars are colored as shown in top legend. A value of 1 means the hydrogen bond is persistent for the entire duration of the trajectory. A hydrogen bond is considered present if the donor-acceptor distance is below 3.5 Å and the acceptor-H-donor angle is less than 120°.



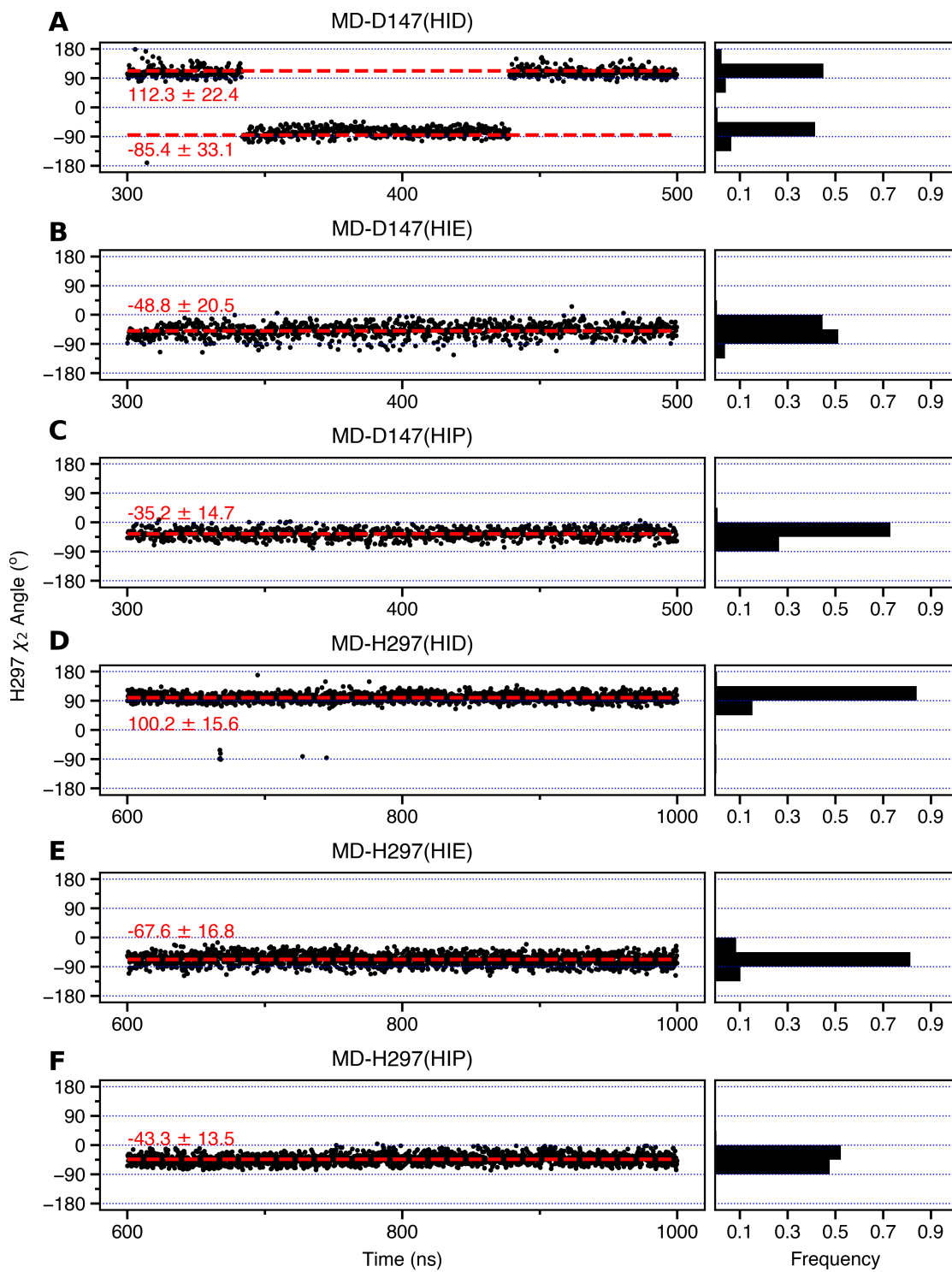
**Supplementary Fig. 8 Fentanyl is pushed away from His297 in the equilibrium simulations of the H297-binding mode with HIE and HIP.** The FEN–H297 distance as a function of simulation time in H297 mode with HID297 (**A**), HIE297 (**B**), and HIP297 (**C**). The FEN–H297 distance is measured between the piperidine nitrogen and the unproto-nated imidazole nitrogen of His297.



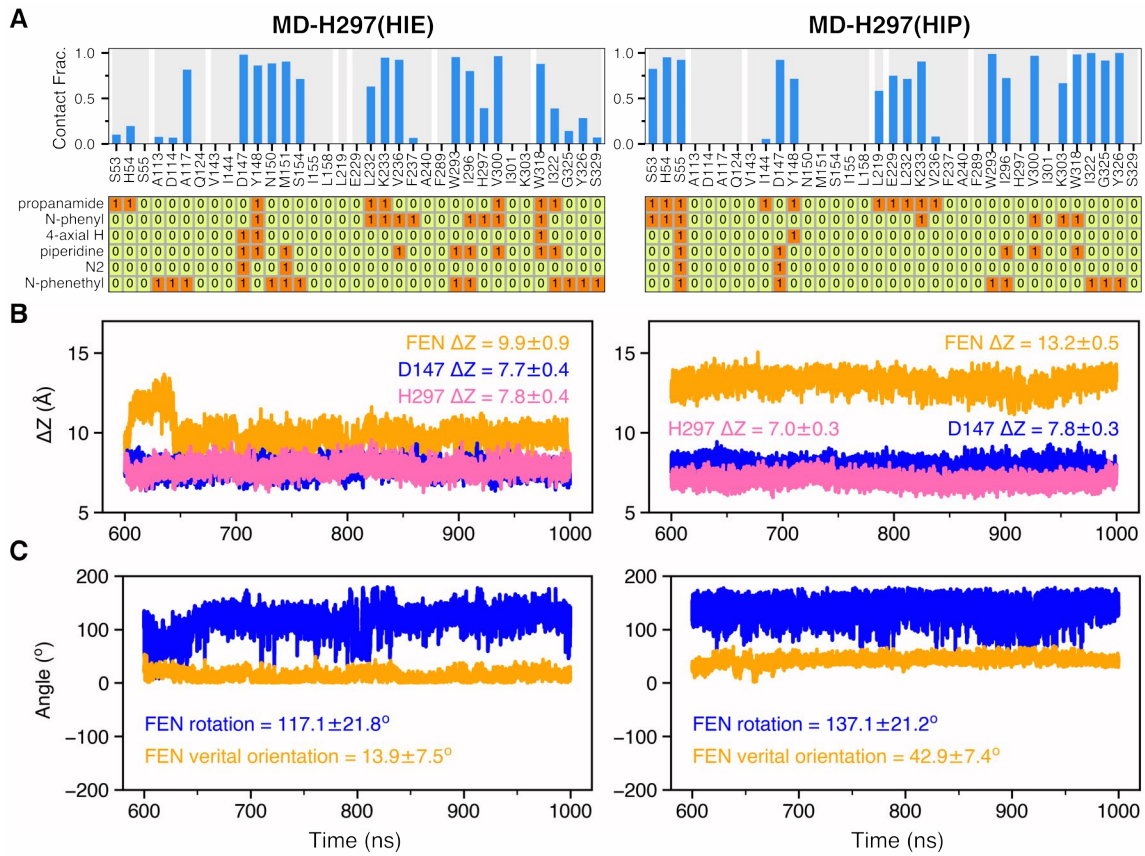
**Supplementary Fig. 9 Trp293  $\chi_2$  angle is somewhat decrease or increased relative to the value ( $120^\circ$ ) in the crystal structure of BU72-bound mOR (PDB 5C1M).<sup>2</sup>** Time series of the Trp293  $\chi_2$  angle in the simulations of the D147- (A-C) and the H297-binding mode (D-F).



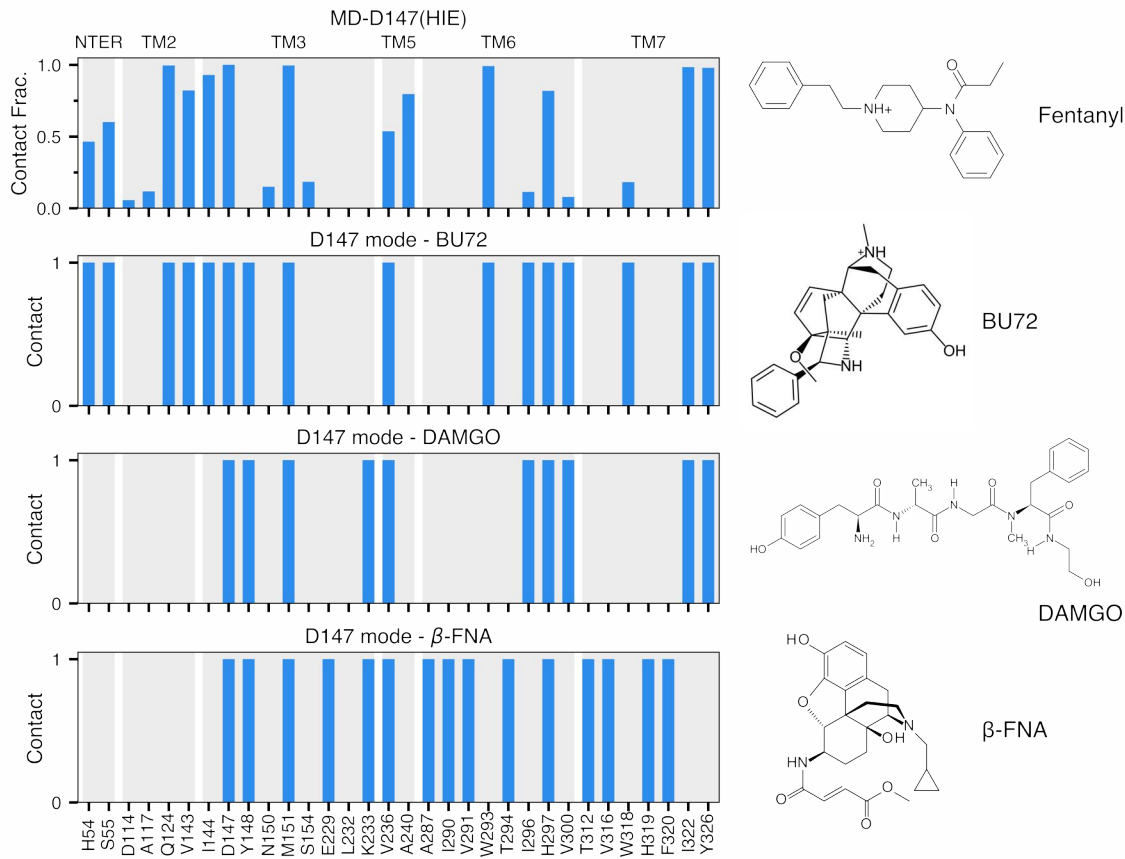
**Supplementary Fig. 10 Fentanyl adopts different orientations in the simulations of the D147- and H297-binding modes.** Time series of the fentanyl rotation angle (blue) and vertical orientation angle (gold). Fentanyl rotation angle is measured by the angle between N2–H vector and the y-axis. Fentanyl vertical orientation angle is measured by the angle between the N2–C4 vector and the membrane normal (z-axis).



**Supplementary Fig. 11 His297's  $\chi_2$  angle is influenced by the protonation/tautomer state.** Time series of the  $\chi_2$  angle of His297 in the simulations of the D147-binding mode (**A-C**) and the H297-binding mode (**D-F**).



**Supplementary Fig. 12 Characterization of the equilibrium simulations of the H297-binding mode with HIE297 and HIP297.** MD-H297(HIE) (left column) and MD-H297(HIP) (right column) simulations. **A.** Fentanyl-mOR contact profile (top) and fingerprint matrix (bottom) from the simulations with HIE297 (left) and HIP297 (right). Details are explained in the caption of Fig. 4 of the main text. **B.** Time series of the vertical positions of fentanyl (gold), Asp147 (blue), and His297 (magenta) from the simulations with HIE297 (left) and HIP297 (right). **C.** Time series of the fentanyl rotation angle (blue) and vertical orientation angle (gold) from the simulations with HIE297 (left) and HIP297 (right). Fentanyl rotation angle is measured by the angle between N2–H vector and the y-axis. Fentanyl vertical orientation angle is measured by the angle between the N2–C4 vector and the membrane normal (z-axis).



**Supplementary Fig. 13 Comparison between fentanyl-mOR contact fraction to the BU72-, DAMGO-,  $\beta$ -FNA-mOR contacts in the crystal structures.** MD-D147(HIE) was shown due to its highest  $T_c$  value compared to BU72 (Figure 5 in the main text). The N-terminal residues (residue 52 to 64) are not resolved in the crystal structures of DAMGO- and  $\beta$ -FNA-mOR.

## References

- (1) Zhang, L.; Hermans, J. Hydrophilicity of Cavities in Proteins. *Proteins* **1996**, *24*, 433.
- (2) Huang, W. et al. Structural Insights into  $\mu$ -Opioid Receptor Activation. *Nature* **2015**, *524*, 315–321.

Reviewer #1 (Remarks to the Author):

Quynh et.al used all-atom long time scaled MD simulations to elaborate the binding process of fentanyl against mu opioid-receptor. Fentanyl is a widely used painkiller and it has been widely studied before.

In my opinion, the biggest disadvantage of this paper is innovation. I found two similar works which were already published in 2019 as following:

(1) Molecular dynamics of fentanyl bound to  $\mu$ -opioid receptor. J Mol Model. 2019 May 3;25(5):144. doi: 10.1007/s00894-019-3999-2

(2) Fentanyl Family at the Mu-Opioid Receptor: Uniform Assessment of Binding and Computational Analysis. Molecules. 2019 Feb; 24(4): 740.

The authors in above mentioned two papers also studied the binding mode of fentanyl against mu opioid receptor. They also used long time scaled MD simulations. The current work here shared a large common results with the above mentioned paper.

Another big concerns is for the pKa calculations which is still one of the biggest challenging in computational biology. I am not so sure how confident the authors about the exact pKa values obtained from MD simulation. It seems that the protonation state is also one of the major points in the work which will bring many concerns.

Some technical details:

- (1) It is not clear to me how the author prepared the crystal structure mu-opioid receptor. In many cases, mutations will be introduced in the biological experiments to stabilize the crystals. Did the author mutate those residues back before MD simulations?
- (2) Which lipids do the authors used for MD simulation? Was cholesterol added to the simulation system?

Reviewer #2 (Remarks to the Author):

In this study by Vo et al., the authors employ weighted ensemble (WE) and continuous constant pH (CpH) molecular dynamics (MD) simulations to analyse how fentanyl, a highly potent opioid, binds to the mu-opioid receptor (mOR). The authors identified two fentanyl binding modes, the latter of which has not been previously observed: (1) the D147 binding mode, in which the fentanyl piperidine amine forms a hydrogen bond (H-bond) with the D147 side chain, and (2) the H297 binding mode, only accessible when H297 is present as the HID tautomer, in which fentanyl protrudes further into mOR and its piperidine amine forms an H-bond with H297.

This study has important implications for our understanding of mOR-fentanyl/opioid interactions and highlights the importance of considering tautomerisation in ligand binding simulations. Overall, the manuscript is very interesting and well-presented. Additionally, the results and figures are well-

described. However, I feel the manuscript could be made stronger and more interesting for a wider audience by addressing the points below. In particular, the scope of the discussion could be expanded, and the significance of the results more clearly conveyed.

#### Major comments

1. A greater discussion of previous studies, which found that fentanyl binding and signalling are pH-independent (Spahn et al., *Science*, 2017; Spahn et al., *Scientific Reports*, 2018; Meyer et al., *Br J Pharmacol*, 2019) would be important (especially the former two studies, which do not report high non-specific binding of fentanyl).
2. The hierarchical clustering analysis (used for Fig 2C,D) is not included in the methods.
3. The authors discuss the sampling of the HID/HIE/HIP states when the fentanyl piperidine nitrogen atom is  $\leq 4$  Å and  $\geq 7$  Å from the His297 Nε (page 4) – what happens when the piperidine nitrogen is  $> 4$  Å and  $< 7$  Å away?
4. It feels slightly misleading when the authors refer to the contacts between fentanyl and residues in TM3,5-7 as conferring “the remarkable stability” to the H297-binding mode (page 5). Fentanyl also forms contacts with many TM3,5-7 residues in the D147-binding mode (as does BU72) (Fig. 4A-C,E). Perhaps this stance could be softened or clarified. The authors could also comment on the fact that most contacts uniquely observed for the fentanyl H297-binding mode appear to be with TM5 residues.
5. The manuscript includes a comparison of the fentanyl and BU72 binding contacts – why are other ligands with solved mOR-bound structures (beta-FNA, DAMGO) not considered?
6. A sizeable amount of the Concluding Discussion is devoted to Asp114, which is not/hardly mentioned in the Results. This section would read more fluidly if the CpHMD simulation results for Asp114 were included in the Results.
7. The claim “it is possible that the H297-binding mode is unique to fentanyl” (page 7) should be strengthened e.g. through more explanation/clarification of how the flexibility of fentanyl enables it to access the H297-binding mode (would the more rigid morphinan ligands be excluded if they are unable to flex in a certain manner?). Furthermore, how does the fentanyl H297-binding mode differ from the morphine binding mode, which forms an H-bond with H297, identified in (Cong et al., *PLOS ONE*, 2015)? Would this morphine binding mode also be classified as an H297-binding mode (thus detracting from the hypothesis that the H297-binding mode is unique to fentanyl)?
8. The manuscript would be strengthened by expanding the scope of the discussion (and if/where needed, analysis) to include points related to some of the following (for example):
  - When/how often is the H297-binding mode achieved? The authors point out that this mode is likely secondary to the D147-binding mode – is it likely to occur only in a negligible amount of cases? If so, would this explain the results of a previous study which found pH-independence for fentanyl signalling (Meyer et al., *Br J Pharmacol*, 2019)? Would there be any conditions (other than fentanyl binding) that favour HID tautomerisation and therefore the H297-binding mode?
  - What would the effects/consequences of the H297-binding mode be e.g. on receptor activation or

fentanyl potency?

- Expanded discussion of how modifications to fentanyl would (or would not) influence the H297-binding mode. Are there any modifications that would prevent the H297-binding mode? How would interpretations of previous results that the affinities of fentanyl derivatives, but not fentanyl, for mOR are pH-sensitive (Spahn et al., Science, 2017; Spahn et al., Scientific Reports, 2018) be influenced by the results presented here of the H297-binding mode?

#### Minor comments

1. It felt, to me, slightly contrived to introduce this study via a link to COVID-19. The opioid crisis is an enormous problem in its own right and, seeing as COVID-19 was not mentioned anywhere else in the text, I feel it could be removed from the Abstract/Introduction.
2. The  $\Delta Z$  score should be more clearly explained when it is first introduced (in the “Fentanyl unbinds from...” paragraph; page 2, top right), e.g. using the explanation included in the Fig 2C,D legend.
3. The HIP tautomer should be defined more clearly in the text (it is mentioned suddenly at one point).
4. Amino acids are denoted in a mixture of single- and three-letter codes (e.g. His297 and H297); it could be preferable to remain consistent.

#### Figure comments

1. It could be helpful to move the structures of the histidine tautomers (Fig 3A) and fentanyl (Fig 4F) to the start of the manuscript (in Fig 1), as this information is highly relevant for understanding the all of the results.
2. For Fig S6, it could be helpful to add a figure showing the frequency of aromatic stacking (0-45° and 135-180° combined) vs. no aromatic stacking.

Alissa M Hummer

#### Reviewer #3 (Remarks to the Author):

In this manuscript, the authors investigated the binding interactions between fentanyl and  $\mu$ -Opioid receptors using a combination of constant-pH and weighted ensemble simulations. They were able to identify the role of protonation of H297 and other conformational changes in the receptor responsible for fentanyl’s changing binding affinity and binding sites. The paper is well written with sufficient details for reproduction of the results and was a pleasure to read. The results are a valuable demonstration of molecular insights that can be obtained for a complex biological process using constant-pH simulations, especially when coupled with an enhanced sampling technique such as the weighted ensemble strategy. Given the current importance of opioid receptors in public health and the compelling molecular insights provided about the binding interactions of these

receptors, I recommend publication of this manuscript in Nature Communications after minor revisions.

My suggestions for minor revisions to further improve the quality of the manuscript are the following:

- 1) Like many contemporary force fields, the CHARMM36 force field overstabilizes protein salt bridges (see Debiec et al. JCTC 2015), which may or may not significantly affect the binding of Fentanyl-D147. I would like to see a comment in the main text or supporting information on the potential effects of this overstabilization issue on the conclusions.
- 2) In the supplementary data (p. S-3), it is listed that "the simulation length for each walker was 0.5 ns". To clarify, is the 0.5 ns the fixed time interval used for resampling in the weighted ensemble strategy? If so, I suggest referring to the 0.5 ns as the fixed time interval for resampling as "simulation length" may be confused with the length of the entire trajectory that consists of multiple fixed time intervals for resampling.
- 3) In the Methods, I assume that a Langevin thermostat was used since the simulations were carried out using the Amber software package. If this is the case, it is worth stating in the Methods that the simulations employed a stochastic thermostat and that this type of thermostat is required for the weighted ensemble strategy to generate continuous pathways with no bias in the dynamics.
- 4) Depending on the number of transition events simulated using WE MD, it may be possible to estimate rate constants for transitions between the two binding modes of HID297 using the approach from Suarez et al. JCTC (2014). This calculation is not essential for the manuscript, but would provide additional valuable insights about the relevant timescales if there is sufficient data to perform the calculations.

Reviewer #4 (Remarks to the Author):

The paper is very well written and nicely illustrated in the main text and also there is a lot of other informative data in the supplementary material. The employed methodologies (the weighted ensemble approach, continuous constant-pH MD with replica-exchange, and classical molecular dynamics) are valid and correctly used for establishing the binding modes and their stabilities of fentanyl in mOR.

Although the paper is interesting it presents only one compound, fentanyl, and no other more potent derivatives, although it is claimed in the paper that "Our work provides a basis for understanding mOR activation by diverse fentanyl derivatives". The receptor activation is also not studied since the receptor structure is already activated.

The binding site for BU72 is very big since the compound is big so the presented double binding mode of fentanyl may be a result of increased binding site of mOR-BU72. It would be good to make a long MD equilibration (about 1us) of empty receptor before docking of fentanyl.

---

We are pleased to submit a revised manuscript entitled “How  $\mu$ -Opioid Receptor Recognizes Fentanyl” by Quynh N. Vo, Paveen Mahinthichaichan, Jana Shen, and Christopher R. Ellis. We would like this work to be reconsidered for publication as a regular article in *Nature Communications*.

We thank the reviewers for their valuable critiques, comments as well as suggestions. We have made revision to the manuscript to fully address and accommodate them. Below we present our response and revision. The revised excerpt is in red and also highlighted in the revised manuscript. Unless otherwise noted, page, table, and figure numbers refer to the revised version.

### **Reviewer #1**

**Reviewer's remark:** *Quynh et.al used all-atom long time scaled MD simulations to elaborate the binding process of fentanyl against mu opioid-receptor. Fentanyl is a widely used painkiller and it has been widely studied before.*

**Response:** We thank the reviewer for recognizing the importance of fentanyl. The reviewer has correctly pointed out the use of all-atom long time scale MD; however, he/she has missed the two other novel computational methodologies used that have made our novel findings possible. Below we give our response and revision to the major and minor comments.

#### **Major comments:**

**Comment 1:** *In my opinion, the biggest disadvantage of this paper is innovation. I found two similar works which were already published in 2019 as following:*

(1) Molecular dynamics of fentanyl bound to mu-opioid receptor. *J Mol Model.* 2019 May 3;25(5):144. doi: 10.1007/s00894-019-3999-2

(2) Fentanyl Family at the Mu-Opioid Receptor: Uniform Assessment of Binding and Computational Analysis. *Molecules.* 2019 Feb; 24(4): 740.

*The authors in above mentioned two papers also studied the binding mode of fentanyl against mu opioid receptor. They also used long time scaled MD simulations. The current work here shared a large common results with the above mentioned paper.*

**Response:** We thank the reviewer for pointing out these two studies, one of which was cited in our original manuscript. We apologize for missing the second reference, which is now added in the revised manuscript in the context of discussing the fentanyl-mOR binding interactions.

**Revision:** Page 5, left column, first paragraph under Figure 3:

The importance of the phenethyl-Tyr293 stacking interaction is also consistent with a recent study which showed that removal of one methylene group from phenethyl increases the IC<sub>50</sub> value by two orders of magnitude (36).

**Revision:** Page 6, right column, last paragraph:

Ref. 36 is added.

**Response:** Regarding the lack of innovation, we respectfully disagree with the reviewer. First, we would like to point out the significant differences in the computational methodologies used in our work vs. the two referenced papers. In the cited papers by Lipiński, Sadlej et al., only conventional equilibrium molecular dynamics (MD) simulations were employed to investigate the binding of mOR with fentanyl and analogs. In the first paper (1), three replicates of 1.2- $\mu$ s conventional MD of fentanyl-mOR complex were conducted, and in the second paper (2), three replicates of 50-ns conventional MD were conducted for each mOR-fentanyl analog complex. All simulations assumed that the titratable sidechains are in the (CHARMM-GUI default) fixed protonation states.

By contrast, our work employed two state-of-the-art MD techniques. 1) Weighted Ensemble (WE) MD is a path sampling method for exploring rare events and larger conformational space. We conducted two sets of WE MD simulations (24  $\mu$ s each) in the presence of different tautomer states of H297. 2) The membrane-enabled continuous constant pH MD (CpHMD) is a method for studying proton-coupled conformational dynamics of transmembrane proteins. We conducted CpHMD to investigate the protonation state of H297 and how it impacts the fentanyl's binding mode.

Next, we would like to point out the new findings from our work which are not reported in the two referenced papers. While we confirmed the stability of the D147-binding mode as in the work of Lipiński, Sadlej et al., our WE MD simulations revealed an alternative binding mode of fentanyl in mOR, which has not been reported before. Furthermore, WE MD revealed that fentanyl's binding mode is dependent on the protonation state of the conserved H297, and CpHMD rationalized this dependence.

In sum, our work is novel, as it employed state-of-the-art MD based methodologies and offered new findings, none of which have been reported in the two publications by Lipiński, Sadlej et al. Finally, we would like to mention that Dr. Lipiński contacted us after seeing our manuscript in bioRxiv and noted that a similar H297 binding mode was also observed in their simulations but the discussion was removed from the publication under the pressure of the skeptical reviewers.

Above being said, to accommodate the reviewer's comment and in light of the communication with Dr. Lipiński, we made the following revision.

**Revision:** Page 8, left column, first paragraph:

These findings are consistent with a recent conventional MD study of the fentanyl-mOR binding, which found that the D147 binding mode was stable in the presence of HID297 (18) but fentanyl moved deeper to contact HID297 in some trajectories (personal communication with Lipiński).

**Comment 2:** Another big concern is for the pKa calculations which is still one of the biggest challenges in computational biology. I am not so sure how confident the authors about the exact pKa values obtained from MD simulation. It seems that the protonation state is also one of the major points in the work which will bring many concerns.

**Response:** We agree with the reviewer that pK<sub>a</sub> calculation is a challenging topic in computational biology. Traditional pK<sub>a</sub> prediction methods are reliant on a single input structure. Over the past 15 years, we and others have been developing MD-based pK<sub>a</sub> methods known as constant pH MD. Notably, the continuous constant pH MD (CpHMD) method which was first developed in the Brooks lab and later in the Shen lab demonstrated significantly improved accuracy for pK<sub>a</sub> calculations over traditional methods (Alexov, Shen et al, Proteins 2011). Importantly, it has enabled for the first time simulations of proton-coupled conformational dynamics of proteins (Khandogin and Brooks, PNAS 2006; PNAS 2007). In more recent years, the method has been widely validated (Chen, Shen et al, Mol Simul 2014) and further developed to enable pK<sub>a</sub> calculations and pH-dependent MD simulations of transmembrane proteins (Huang, Shen et al, Nat Commun 2016; Chen, Shen et al, J Phys Chem Lett; Henderson, Shen et al, PNAS 2020). The latter method, the membrane-

enabled CpHMD forms a basis of this work.

The reviewer is correct in that the protonation state is a major point in this work. It has been shown through both experiments and MD simulations that H297 plays an important role in mOR-ligand binding; however, the nature of the role remains unknown. Our work revealed a novel mechanism by which H297 can influence mOR-ligand binding and demonstrated the limitation of conventional MD simulations based on a single protonation state. The CpHMD method was briefly explained in the SI with proper references. To accommodate the reviewer's comment, we added a sentence about the membrane-enabled CpHMD method in Introduction.

**Revision:** Page 1, right column, last paragraph:

The latter method has been previously applied to calculate  $pK_a$ 's and describe proton-coupled conformational dynamics of membrane channels (25) and transporters (23,26,27).

**Minor comments:**

**Comment 1:** *It is not clear to me how the author prepared the crystal structure mu-opioid receptor. In many cases, mutations will be introduced in the biological experiments to stabilize the crystals. Did the author mutate those residues back before MD simulations?*

**Response:** The preparation of the simulation system using the crystal structure of  $\mu$ OR (PDB 5C1M) is described in the SI:

"The crystal structure of mOR in complex with BU72 was used as the starting model for apo active mOR. All crystal waters in the interior of mOR were kept, and seven additional water molecules were added using the DOWSER program. Apo mOR was oriented with respect to membrane using the OPM (Orientations of Proteins in Membranes) database..."

The crystal structure represents the wild type and contains a cysteine-s-acetamide (YCM) at position 57. This residue was converted to a cysteine (Cys57), and there was no further mutation. We added a description in the SI regarding this point.

**Revision:** SI page S-2, first paragraph:

The crystal structure represents the wild type mOR but contains a cysteine-s-acetamide (YCM) at position 57. This residue was converted back to a cysteine (Cys57).

**Comment 2:** *Which lipids do the authors used for MD simulation? Was cholesterol added to the simulation system?*

**Response:** POPC (1-palmitoyl-2-oleoyl-glycero-3-phosphocholine) lipid was used. There is one cholesterol molecule in the simulation system. This molecule was resolved in the crystal structure (PDB 5C1M) and is bound to the extracellular leaflet near TM7.

To clarify these points, we revised the corresponding sentences in the SI.

**Revision:** SI page S-2, first paragraph:

A cholesterol molecule was resolved in the X-ray structure and is bound to the extracellular leaflet near TM7. This cholesterol and all crystal waters in the interior of mOR were kept.

**Revision:** SI page S-2, first paragraph:

... mOR embedded in POPC (1-palmitoyl-2-oleoyl-glycero-3-phosphocholine) lipid bilayer.

## Reviewer #2

**Reviewer's remark:** *In this study by Vo et al., the authors employ weighted ensemble (WE) and continuous constant pH (CpH) molecular dynamics (MD) simulations to analyse how fentanyl, a highly potent opioid, binds to the mu-opioid receptor (mOR). The authors identified two fentanyl*

*binding modes, the latter of which has not been previously observed: (1) the D147 binding mode, in which the fentanyl piperidine amine forms a hydrogen bond (H-bond) with the D147 side chain, and (2) the H297 binding mode, only accessible when H297 is present as the HID tautomer, in which fentanyl protrudes further into mOR and its piperidine amine forms an H-bond with H297. This study has important implications for our understanding of mOR-fentanyl/opioid interactions and highlights the importance of considering tautomerisation in ligand binding simulations. Overall, the manuscript is very interesting and well-presented. Additionally, the results and figures are well-described. However, I feel the manuscript could be made stronger and more interesting for a wider audience by addressing the points below. In particular, the scope of the discussion could be expanded, and the significance of the results more clearly conveyed.*

**Response:** We thank the reviewer for the favorable view of the paper and the detailed comments. Below we give our response and revision.

**Major comments:**

**Comment 1:** *A greater discussion of previous studies, which found that fentanyl binding and signalling are pH-independent (Spahn et al., Science, 2017; Spahn et al., Scientific Reports, 2018; Meyer et al., Br J Pharmacol, 2019) would be important (especially the former two studies, which do not report high non-specific binding of fentanyl).*

**Response:** To address this comment, we expanded the discussion.

**Revision:** Page 8, left column, third paragraph:

This hypothesis is consistent with the recent experiments (15,44,45) showing that acidic pH has a negligible effect on fentanyl-mOR binding. These experiments also showed that fluorinated fentanyl which have lower  $pK_a$ 's (6.8–7.2) than fentanyl ( $\sim 8.9$ ) (46,47) have increased affinities for mOR at lower pH. The CpHMD simulations showed that fentanyl's piperidine amine remains protonated/charged up to pH 9.5, while Asp147 is deprotonated with an estimated  $pK_a$  of 3–4. Thus, our data is consistent with the hypothesis (44,45,48) that while fentanyl's D147-binding is not affected, lowering pH promotes protonation of the fluorinated fentanyls and thereby strengthening the salt bridge with Asp147. We expect the fluorinated fentanyls to have a lower potential for the His297-binding mode at physiological pH than fentanyl due to the decreased protonation of the piperidine.

**Comment 2:** *The hierarchical clustering analysis (used for Fig 2C,D) is not included in the methods.*

**Response:** Description of the clustering method is now added to the SI.

**Revision:** SI page S-5, bottom:

The clustering analysis was performed using the cluster command in CPPTRAJ program with the hierarchical agglomerate algorithm. The distance between clusters was calculated based on the RMSD of fentanyl's heavy atoms. The distance cutoff was 3 Å.

**Comment 3:** *The authors discuss the sampling of the HID/HIE/HIP states when the fentanyl piperidine nitrogen atom is  $\leq 4$  Å and  $\geq 7$  Å from the His297 N $\epsilon$  (page 4) – what happens when the piperidine nitrogen is  $> 4$  Å and  $< 7$  Å away?*

**Response:** As can be seen from Figure 3D, fentanyl rarely samples distances of 4–7 Å between its piperidine amine and His297 residue. This observation is consistent with equilibrium MD simulations in which the distance is  $3.0 \pm 0.22$  Å when His297 is in the HID tautomer, or  $7.4 \pm 0.72$  Å and  $8.0 \pm 0.5$  Å when His297 is in HIE or HIP form, respectively (Figure S8). We added the clarification in the main text.

**Revision:** Page 3, left column, second paragraph:

The CpHMD data is consistent with the equilibrium MD which shows that the distance is  $3.0 \pm 0.22$  Å,  $7.4 \pm 0.72$  Å, and  $8.0 \pm 0.5$  Å with HID297, HIE297, and HIP297, respectively, while the distance range 4–7 Å is rarely sampled (Fig. S8). Note, in both holo simulations the piperidine amine remains protonated/charged in the entire pH range 2.5–9.5.

**Comment 4:** *It feels slightly misleading when the authors refer to the contacts between fentanyl and residues in TM3,5-7 as conferring “the remarkable stability” to the H297-binding mode (page 5). Fentanyl also forms contacts with many TM3,5-7 residues in the D147-binding mode (as does BU72) (Fig. 4A-C,E). Perhaps this stance could be softened or clarified. The authors could also comment on the fact that most contacts uniquely observed for the fentanyl H297-binding mode appear to be with TM5 residues.*

**Response:** We deemed the H297-binding mode as “remarkably stable” because all the contacts within H297-binding mode, except with Asp147, have a contact fraction greater than 0.5. Nonetheless, we have softened the language used in the text to describe the H297-binding mode and commented on TM5 contacts as suggested by the reviewer.

**Revision:** Page 5, right column, second paragraph:

... the simulation MD-H297(HID) shows that fentanyl forms stable contacts (**with a contact fraction greater than 0.5**) with over a dozen of residues ..., which explains the stability of the H297-binding mode ...

**Revision:** Page 5, right column, last paragraph:

**Most contacts uniquely observed for the H297-binding mode involve TM5 residues.**

**Comment 5:** *The manuscript includes a comparison of the fentanyl and BU72 binding contacts – why are other ligands with solved mOR-bound structures (beta-FNA, DAMGO) not considered?*

**Response:** We only compared the binding profile of fentanyl with the BU72-mOR complex structure, as it was used as a template to build the initial structure of fentanyl-mOR complex for WE simulations. We also note that both  $\beta$ -FNA (Huang et al., Nature 2015) and DAMGO (Koehl et al., Nature 2018) have been shown to occupy the same binding pocket and adopt similar bound poses as BU72.

To clarify these points, we made revision to the main text and added a new contact plot in the SI that compares fentanyl-mOR binding profile with the contact profiles of BU72, DAMGO, and  $\beta$ -FNA based on the X-ray structures.

**Revision:** Page 7, right column, third paragraph:

**Comparison to the X-ray structures of mOR in complex with BU72 and other ligands.** Finally, we compare the two fentanyl binding modes to the crystal structure of the BU72-bound mOR, which was used as a template to build the initial structure of fentanyl-mOR complex for WE simulations...

In addition to BU72, we compare fentanyl’s D147-binding profile (HIE297) to DAMGO- and  $\beta$ -FNA contacts with mOR based on the crystal structures (Fig. S13). In contrast to fentanyl and BU72, DAMGO (a natural agonist) and  $\beta$ -FNA (an antagonist) do not form contacts with TM2 in the crystal structures. Other than that, DAMGO-mOR contact profile is similar to BU72-mOR and fentanyl’s D147-binding profile (with HIE297), whereas  $\beta$ -FNA makes additional contacts with TM6 (Ala287, I290, and V291) and has different contacts with TM7.

**Revision:** SI Page S-21:

Figure S13 is added.

**Comment 6:** *A sizeable amount of the Concluding Discussion is devoted to Asp114, which is not/hardly mentioned in the Results. This section would read more fluidly if the CpHMD simulation*

results for Asp114 were included in the Results.

**Response:** We added a discussion regarding Asp114 in Results and Discussion and significantly shortened the related discussion in Concluding Discussion.

**Revision:** Page 3, right column, last paragraph:

**Asp114 is deprotonated.** The protonation state of the highly conserved residue Asp114 (Asp<sup>2.50</sup>) in the active mOR remains unclear to this day. Despite not having a direct role in ligand binding, Asp114 is involved in mOR activation (9,11,29,30). Previous experiments (30) and simulations (9,11,29) demonstrated that Asp114 binds a sodium ion in the inactive but not active state of GPCRs. Based on the lack of sodium binding, two previous MD studies used a protonated Asp114 (9,11), while other published work did not specify the protonation state (18,31,32). The CpHMD titration gave a  $pK_a$  of  $4.8 \pm 0.30$  for the apo and  $5.1 \pm 0.26/0.29$  for the holo active mOR in the D147- or H297-binding mode. Therefore, even though the  $pK_a$ 's are upshifted relative to the solution value of 3.8 (33), Asp114 remains deprotonated at physiological pH in the active mOR according to the CpHMD simulations.

**Revision:** Page 8, right column, second paragraph:

The CpHMD titration allowed us to determine the protonation states of His297 and all other titratable sites in mOR, including the conserved Asp114<sup>2.50</sup>. Sodium binding in the inactive mOR suggests a deprotonated Asp114 (30), while the protonation state for the active mOR remains unclear...

The CpHMD simulations estimated the  $pK_a$ 's of 4.8–5.1 for the apo and fentanyl-bound mOR, thus suggesting that it remains deprotonated in the active mOR.

**Comment 7:** *The claim “it is possible that the H297-binding mode is unique to fentanyl” (page 7) should be strengthened e.g. through more explanation/clarification of how the flexibility of fentanyl enables it to access the H297-binding mode (would the more rigid morphinan ligands be excluded if they are unable to flex in a certain manner?). Furthermore, how does the fentanyl H297-binding mode differ from the morphine binding mode, which forms an H-bond with H297, identified in (Cong et al., PLOS ONE, 2015)? Would this morphine binding mode also be classified as an H297-binding mode (thus detracting from the hypothesis that the H297-binding mode is unique to fentanyl)?*

**Response:** Our work showed that fentanyl can bind via either D147 or H297 but not at the same time. This is in contrast to the crystal structures and simulations of morphinan ligands, which bind mOR via the D147-binding mode, while forming a water-mediated hydrogen bond with H297 at the same time (Cong et al, PLOS ONE, 2015; Huang et al, Nature 2915; Koehl et al, Nature 2018).

To clarify this point and expand on the discussion of the differences between fentanyl and morphinan ligands which may lead to the unique H297 binding mode, we made the following revision.

**Revision:** Page 8, left column, last paragraph:

The X-ray structures of mOR in complex with BU72,  $\beta$ -FNA, and DAMGO (9-11) show that while the piperidine amine forms a salt bridge with Asp147, the phenol hydroxyl group of the ligand forms a water-mediated hydrogen bond with His297. MD simulations of Dror and coworkers confirmed the stability of the water-mediated interactions between BU72 or DAMGO and His297 (HIE). (9,11) Simulations of Carloni and coworkers (31) found that while in the D147-binding mode, the phenol group of morphine or hydromorphone forms a direct or water-mediated hydrogen bond with His297 (HIE), respectively. Morphine was also suggested to make hydrophobic contacts with His297 (HID) while in the D147-binding mode by the recent MD study of Lipiński and Sadlej. (18) The de novo binding simulations of the Filizola group (32) showed that oliceridine (TRV-130) which has an atypical chemical scaffold binds mOR via water-mediated interactions with Asp147, while frequently contacting His297 (protonation state unclear). Fentanyl does not have a phenol group, and it differs from morphinan ligands in several other ways. Fentanyl has an elongated shape;

it is highly flexible with at least seven rotational bonds; and it has only two structural elements capable of forming hydrogen bonds (amine and carbonyl groups). In contrast, morphinan ligands are bulkier, rigid, and possess more structural elements (i.e. phenol group) with hydrogen bonding capabilities. The bulkier structure and additional hydrogen bond interactions may further stabilize the piperidine-D147 salt bridge, preventing the ligand from moving deeper into mOR and access the H297-binding mode. Therefore, it is possible that the H297-binding mode is unique to fentanyl and analogs.

**Comment 8:** *The manuscript would be strengthened by expanding the scope of the discussion (and if/where needed, analysis) to include points related to some of the following (for example):*

- *When/how often is the H297-binding mode achieved? The authors point out that this mode is likely secondary to the D147-binding mode – is it likely to occur only in a negligible amount of cases? If so, would this explain the results of a previous study which found pH-independence for fentanyl signalling (Meyer et al., Br J Pharmacol, 2019)? Would there be any conditions (other than fentanyl binding) that favour HID tautomerisation and therefore the H297-binding mode?*
- *What would the effects/consequences of the H297-binding mode be e.g. on receptor activation or fentanyl potency?*
- *Expanded discussion of how modifications to fentanyl would (or would not) influence the H297-binding mode. Are there any modifications that would prevent the H297-binding mode? How would interpretations of previous results that the affinities of fentanyl derivatives, but not fentanyl, for mOR are pH-sensitive (Spahn et al., Science, 2017; Spahn et al., Scientific Reports, 2018) be influenced by the results presented here of the H297-binding mode?*

**Response to comment 8.1:** Our CphMD simulations showed that for the apo mOR, HIE is the dominant state at physiological pH, whereas the population for HID is only 12%. That's the reason why we hypothesized that the H297-binding mode is secondary to the D147-binding mode. However, the WE simulation was not long enough in order for us to estimate the relative free energy of the two binding modes. To clarify this point, we added a discussion.

The reviewer is correct in that the D147-binding mode being primary is consistent with the experiment of Meyer, Stein, et al (Meyer et al., Br J Pharmacol, 2019), which showed that fentanyl has a similar affinity for mOR at pH 6, 6.5 and 7.4, although the fraction of unspecific binding is very high. As to whether there is a condition that would favor HID tautomer and thereby the H297-binding mode, we do not know the answer and we do not think it is appropriate to make a speculation in the absence of any data.

**Revision:** Page 8, left column, second paragraph:

We note that calculation of the relative stability of the D147- vs. H297-binding mode is beyond the scope of the present work. Such a study would require converged WE simulations and accurate force field for quantifying the strengths of salt bridges and hydrogen bonds...

**Response to comment 8.2:** We did not observe any significant changes to the receptor conformation during the 1- $\mu$ s equilibrium MD simulation of the H297-binding mode. That said, if there was any effect, it would likely occur on a much longer timescale. Thus, we cannot comment on the effect of the H297-binding mode on receptor activation. We added a brief discussion to reflect this point. We would need free energy data in order to comment on the potency, but it is beyond the scope of this work.

**Revision:** Page 9, left column, first paragraph:

We also note that the present work is based on the activated structure of mOR and does not explore the large conformational changes of the receptor, which likely occur on a much slower timescale, e.g., the activation time of the class A GPCR  $\alpha_{2A}$  adrenergic receptor was estimated as 40 ms (55).

**Response to comment 8.3:** Stein and coworkers hypothesized that the pH-sensitive affinities

of the fentanyl derivatives FF3 and NFEPP are due to the pH-modulated piperidine-D147 salt bridge interaction. Specifically, these compounds (piperidine amines) have solution  $pK_a$ 's below physiological pH 7.4, and thus the salt bridge is intact at low pH but may be weakened or disrupted at physiological pH. Deprotonation of piperidine would prevent it from donating a hydrogen bond to H297. Thus, we expect these compounds to have a lower potential to access the H297-binding mode at physiological pH.

**Revision:** Page 8, left column, second paragraph from the bottom:

This hypothesis is consistent with the recent experiments (15,44,45) showing that acidic pH has a negligible effect on fentanyl-mOR binding. These experiments also showed that fluorinated fentanyl which have lower  $pK_a$ 's (6.8–7.2) than fentanyl (~8.9) (46,47) have increased affinities for mOR at lower pH. The CpHMD simulations showed that fentanyl's piperidine amine remains protonated/charged up to pH 9.5, while Asp147 is deprotonated with an estimated  $pK_a$  of 3–4. Thus, our data is consistent with the hypothesis (44,45,48) that while fentanyl's D147-binding is not affected, lowering pH promotes protonation of the fluorinated fentanyls and thereby strengthening the salt bridge with Asp147. We expect the fluorinated fentanyls to have a lower potential for the His297-binding mode at physiological pH than fentanyl due to the decreased protonation of the piperidine.

#### **Minor comments:**

**Comment 1:** *It felt, to me, slightly contrived to introduce this study via a link to COVID-19. The opioid crisis is an enormous problem in its own right and, seeing as COVID-19 was not mentioned anywhere else in the text, I feel it could be removed from the Abstract/Introduction.*

**Response:** To accommodate the reviewer's comment, we have removed the text related to COVID-19 from the Abstract and Introduction.

**Revision:** Page 1, left column, Abstract:

Drug overdose has claimed over 70,000 lives in the United States in 2019.

**Revision:** Page 1, left column, first paragraph:

From 1999–2018, almost 450,000 people died from opioid overdose in the United States (1).

**Comment 2:** *The  $\Delta Z$  score should be more clearly explained when it is first introduced...*

**Response:** We revised the definition as suggested by the reviewer.

**Revision:** Page 2, left column, second paragraph:

$\Delta Z$  is defined as the distance between the centers of mass (COM) of fentanyl and mOR in the z direction, whereby the N- (52–65) and C-terminal (336–347) residues were excluded from the calculation.

**Comment 3:** *The HIP tautomer should be defined more clearly in the text (it is mentioned suddenly at one point).*

**Response and Revision:** HIP tautomer is now better defined in the updated Figure 1.

**Comment 4:** *Amino acids are denoted in a mixture of single- and three-letter codes (e.g. His297 and H297); it could be preferable to remain consistent.*

**Response and Revision:** The text has been edited throughout to be consistent.

#### **Figure comments:**

**Comment 1:** *It could be helpful to move the structures of the histidine tautomers (Fig 3A) and fentanyl (Fig 4F) to the start of the manuscript (in Fig 1), as this information is highly relevant for understanding the all of the results.*

**Response and Revision:** Figure 1 has been updated as suggested by the reviewer.

**Comment 2:** For Fig S6, it could be helpful to add a figure showing the frequency of aromatic stacking ( $0\text{-}45^\circ$  and  $135\text{-}180^\circ$  combined) vs. no aromatic stacking.

**Response and Revision:** Figure S6 has been revised to include a new panel as suggested by the reviewer.

### Reviewer #3

**Reviewer's remark:** In this manuscript, the authors investigated the binding interactions between fentanyl and mu-Opioid receptors using a combination of constant-pH and weighted ensemble simulations. They were able to identify the role of protonation of H297 and other conformational changes in the receptor responsible for fentanyl's changing binding affinity and binding sites. The paper is well written with sufficient details for reproduction of the results and was a pleasure to read. The results are a valuable demonstration of molecular insights that can be obtained for a complex biological process using constant-pH simulations, especially when coupled with an enhanced sampling technique such as the weighted ensemble strategy. Given the current importance of opioid receptors in public health and the compelling molecular insights provided about the binding interactions of these receptors, I recommend publication of this manuscript in *Nature Communications* after minor revisions.

**Response:** We thank the reviewer for the favorable view of the paper and the helpful comments/suggestions. Below we give our response and revision to the minor comments.

#### Minor comments:

**Comment 1:** Like many contemporary force fields, the CHARMM36 force field overstabilizes protein salt bridges (see Debiec et al. JCTC 2015), which may or may not significantly affect the binding of Fentanyl-D147. I would like to see a comment in the main text or supporting information on the potential effects of this overstabilization issue on the conclusions.

**Response:** We agree with the reviewer that the CHARMM36 and CHARMM36m (used in the fixed-charge simulations of the present work) force field overstabilize salt bridges. We added a brief discussion with a citation to the paper by Debiec, Chong, et al.

**Revision:** Page 8, left column, second paragraph:

Previous work by us (25) and others (40) showed that the CHARMM36 (41) or the CHARMM36m force field (42) used in this work overstabilizes salt bridges formed by aspartates, although this might not be the case for the piperidine-Asp147 interaction. Overstabilization of salt bridges is a common problem of additive force fields, which may be overcome by explicit or implicit consideration of polarization (40).

**Comment 2:** In the supplementary data (p. S-3), it is listed that "the simulation length for each walker was 0.5 ns". To clarify, is the 0.5 ns the fixed time interval used for resampling in the weighted ensemble strategy? If so, I suggest referring to the 0.5 ns as the fixed time interval for resampling as "simulation length" may be confused with the length of the entire trajectory that consists of multiple fixed time intervals for resampling.

**Response:** The text has been edited as recommended by the reviewer.

**Revision:** Page S-4, first paragraph.

The fixed time interval for resampling of each walker was 0.5 ns

**Comment 3:** In the Methods, I assume that a Langevin thermostat was used since the simulations were carried out using the Amber software package. If this is the case, it is worth stating in the Methods that the simulations employed a stochastic thermostat and that this type of thermostat is

*required for the weighted ensemble strategy to generate continuous pathways with no bias in the dynamics.*

**Response:** The reviewer is correct in that the Langevin thermostat was used, as stated on page S-5 in the paragraph **Molecular dynamics protocol**. To emphasize this, we have added a sentence in the paragraph Weighted ensemble MD simulations.

**Revision:** SI page S-4, first paragraph.

The WE simulations employed the Langevin thermostat, as a stochastic thermostat is required to for the WE strategy to generate continuous pathways with no bias in the dynamics.

**Comment 4:** *Depending on the number of transition events simulated using WE MD, it may be possible to estimate rate constants for transitions between the two binding modes of HID297 using the approach from Suarez et al. JCTC (2014). This calculation is not essential for the manuscript, but would provide additional valuable insights about the relevant timescales if there is sufficient data to perform the calculations.*

**Response:** We agree with the reviewer that an estimation of the rate constants for transitions between the two binding modes would give valuable insights. However, we do not have sufficient data at this point. We added a clarification in Concluding Discussion and cited the suggested reference.

**Revision:** Page 8, left column, second paragraph:

We also note that given converged WE simulations, the transition rate between the two binding modes may be estimated (43), which is a topic of future study.

## Reviewer #4

**Reviewer's remark:** *The paper is very well written and nicely illustrated in the main text and also there is a lot of other informative data in the supplementary material. The employed methodologies (the weighted ensemble approach, continuous constant-pH MD with replica-exchange, and classical molecular dynamics) are valid and correctly used for establishing the binding modes and their stabilities of fentanyl in mOR.*

**Response:** We thank the reviewer for the favorable view of the paper and insightful comments. Below we give our response and revision.

**Comment 1:** *Although the paper is interesting it presents only one compound, fentanyl, and no other more potent derivatives, although it is claimed in the paper that "Our work provides a basis for understanding mOR activation by diverse fentanyl derivatives". The receptor activation is also not studied since the receptor structure is already activated.*

**Response:** We agree with the reviewer that the particular sentence in the Introduction might be misleading, as the paper only discusses fentanyl and its binding modes without considering the receptor conformational changes. That being said, what we meant is that our study provides a starting point for understanding how fentanyl activates mOR at a molecular level, as until now no crystal structure of mOR bound to fentanyl or analogs has been determined. A direct molecular dynamics simulation of the mOR activation by fentanyl is likely unfeasible, given the three orders of magnitude difference between the simulation and experimental time scale, e.g., the activation time of the class A GPCR  $\alpha_{2A}$  adrenergic receptor was estimated as 40 ms ( Vilardaga, Lohse et al., Nat.Biotechnol. 2003).

To address the reviewer's comment and clarify the above points, we revised the related text.

**Revision:** In Abstract:

Our work provides a starting point for understanding the molecular basis of mOR activation by

fentanyl which has many analogs emerging at a rapid pace.

**Revision:** Page 1, right column:

Our work provides a starting point for understanding how fentanyl activates mOR at a molecular level. Fentanyl analogs that can be significantly more potent and addictive than fentanyl are emerging on the dark market at a rapid pace.

**Revision:** Page 9, left column, first paragraph:

We also note that the present work is based on the activated structure of mOR and does not explore the large conformational changes of the receptor, which likely occur on a much slower timescale, e.g., the activation time of the class A GPCR  $\alpha_{2A}$  adrenergic receptor was estimated as 40 ms (55). Notwithstanding the caveats, our detailed fentanyl-mOR interaction fingerprint analysis provides a basis for pharmacological investigations of fentanyl analogs, particularly how structural modifications alter the binding properties of newly identified fentanyl derivatives which may have increased potency and abuse potential.

**Comment 2:** *The binding site for BU72 is very big since the compound is big so the presented double binding mode of fentanyl may be a result of increased binding site of mOR-BU72. It would be good to make a long MD equilibration (about 1us) of empty receptor before docking of fentanyl.*

**Response:** The reviewer has raised an interesting point. In order to address this comment, we performed the binding pocket volume calculations using the crystal structure of the BU72-bound mOR and snapshots from the trajectory of the apo mOR simulation. After 110 ns, the volume stayed similar to the value from the crystal structure; however, after 500 ns, the volume increased from  $359 \pm 12$  to  $465 \pm 51 \text{ \AA}^3$ . Thus, prolonged apo simulation would not reduce the binding site volume. Note, we would not prolong the simulation even further, as without a bound agonist, the active structure might relax towards the inactive state. We have added the calculations and discussion in the SI.

**Revision:** SI, page S-6: A reviewer noted that BU72 is big and so the second binding mode may be the result of using the BU72-bound mOR crystal structure as a template to generate the initial structure for the fentanyl-mOR complex. The reviewer suggested running a  $1-\mu\text{s}$  MD equilibration of the empty receptor (with the goal to “shrink the binding pocket”). To address this comment, we performed the binding site volume calculations using POVME2.0 (S27, S28). All structures were first aligned using the binding site residues identified from the BU72-bound mOR crystal structure (PDB ID: 5C1M). All waters, ions, cholesterol, lipids, nanobody, and ligands were removed before the calculation. The binding pocket searching region is kept consistent throughout all systems by specifying an Inclusion box centered at the binding pocket center of mass (0,0,8) and sides of 12, 12, 15  $\text{\AA}$  in the x, y, and z direction, respectively.

The binding site volume based on the BU72-bound mOR crystal structure (with BU72 removed) is  $371 \text{ \AA}^3$ . After 110 ns of MD equilibration before docking fentanyl, the volume is  $359 \pm 12 \text{ \AA}^3$ , which is similar to that from the crystal structure. To test if prolonged equilibration would shrink the binding site volume, we extended the simulation by 500 ns and found that the receptor’s cavity volume increased to  $465 \pm 51 \text{ \AA}^3$ . An increase in volume can be rationalized as the result of relaxation and solvation of the binding site. Thus, a long MD equilibration of the empty receptor will not reduce the binding site volume, and the alternative binding mode of fentanyl is not a result of an expanded binding cavity due to the size of BU72.

We thank the reviewers again for their insightful comments, criticism, and suggestions. We have revised the manuscript to fully address and accommodate them. As a result, we believe the revised

manuscript is significantly improved and ready to be accepted.

Sincerely,

Jana Shen  
Professor, Codirector,  
Computer-Aided Drug Design  
Center, American Chemical Society,  
COMP Division Chair Elect 2021  
Dept of Pharmaceutical Sciences  
University of Maryland School of  
Pharmacy, Baltimore, MD

Reviewer #1 (Remarks to the Author):

My major concerns on the innovation of this work were totally ignored. The author only simply cited the already published two similar works and didn't clarify what exactly new and innovations in the current work.

I am pretty disappointed by this. Thus, I won't suggest for publication.

Reviewer #2 (Remarks to the Author):

The authors have, in my view, appropriately and sufficiently addressed all the reviewer comments. To reiterate from my previous report, the manuscript has multiple novel findings which could impact future research, including:

1. A better understanding of fentanyl binding to mOR, as well as the identification of a novel binding mode, which could influence our understanding of the binding of fentanyl analogs and other ligands to mOR.
2. An emphasis on the importance of investigating tautomerization states with regards to receptor/protein-ligand interactions.

One potential limitation is that, from this work alone, it is difficult to estimate how significant the alternative His297-binding mode of fentanyl is under physiological conditions. However, given the role of fentanyl in the opioid crisis and the possibility that this alternative binding mode could influence mOR-mediated responses to fentanyl, the findings in this work are meaningful. Additionally, this work will hopefully spur further research into the physiological prevalence and effects of the alternative fentanyl binding mode, as well as into the binding modes of fentanyl analogs and other mOR ligands.

In light of all these points, I fully support the acceptance of this manuscript.

Alissa M Hummer

Reviewer #4 (Remarks to the Author):

The Authors correctly and carefully replied to all the concerns and made the required additional MD simulation. The results confirm their initial findings therefore an existence of an additional binding mode of fentanyl presented in the paper is strengthened.

We are pleased to submit a revised manuscript entitled "How  $\mu$ -Opioid Receptor Recognizes Fentanyl" by Quynh N. Vo, Paveen Mahinthichaichan, Jana Shen, and Christopher R. Ellis. We would like this work to be reconsidered for publication as a regular article in *Nature Communications*. We thank the reviewers for reading our response and revision. Below we present our response to the reviewers' new remarks.

#### **Reviewer #1**

**Remarks to the Author:** *My majors concerns on the innovation of this work were totally ignored. The author only simply cited the already published two similar works and didn't clarified what exactly new and innovations in the current work.*

*I am pretty disappointed by this. Thus, I won't suggest for publication.*

**Response:** We are very surprised by the remark of this reviewer. In our previous response letter, we explained in detail how our work differs from the previous two publications in both methodologies and findings. The differences are also explained in the manuscript. Furthermore, the first author of these previous publications (Dr. Lipínski) remarked on the novelty of our work and recommended publication, and so did the other three reviewers. Thus, we find the reviewer's concern unjustified and we respectfully disagree with it.

#### **Reviewer #2**

**Remarks to the Author:** *The authors have, in my view, appropriately and sufficiently addressed all the reviewer comments. To reiterate from my previous report, the manuscript has multiple novel findings which could impact future research, including:*

1. *A better understanding of fentanyl binding to mOR, as well as the identification of a novel binding mode, which could influence our understanding of the binding of fentanyl analogs and other ligands to mOR.*
2. *An emphasis on the importance of investigating tautomerization states with regards to receptor/protein-ligand interactions.*

*One potential limitation is that, from this work alone, it is difficult to estimate how significant the alternative His297-binding mode of fentanyl is under physiological conditions. However, given the role of fentanyl in the opioid crisis and the possibility that this alternative binding mode could influence mOR-mediated responses to fentanyl, the findings in this work are meaningful. Additionally, this work will hopefully spur further research into the physiological prevalence and effects of the alternative fentanyl binding mode, as well as into the binding modes of fentanyl analogs and other mOR ligands.*

*In light of all these points, I fully support the acceptance of this manuscript.*

**Response:** We thank the reviewer for reading our response and revision. We also appreciate the reviewer's summary and recommendation of publication.

#### **Reviewer #4**

**Remarks to the Author:** *The Authors correctly and carefully replied to all the concerns and made the required additional MD simulation. The results confirm their initial findings therefore an existence of an additional binding mode of fentanyl presented in the paper is strengthened.*

**Response:** We thank the reviewer for reading our response and revision.

In summary, we have made revision to fully accommodate the reviewers' critiques and comments. We hope the manuscript is ready to be accepted for publication.